CHARACTERIZATION OF THE CHICKEN TRANSCRIPTOME AND DIFFERENTIAL MORPHOMETRIC GROWTH IN MODERN BROILER CHICKENS AND A HERITAGE LINE

by

Brooke Enslen

A thesis submitted to the Faculty of the University of Delaware in partial fulfillment of the requirements for the degree of Master of Science in Animal Sciences

Fall 2013

CHARACTERIZATION OF THE CHICKEN TRANSCRIPTOME AND DIFFERENTIAL MORPHOMETRIC GROWTH IN MODERN BROILER CHICKENS AND A HERITAGE LINE

by

Brooke Enslen

Approved: _____
Carl Schmidt, Ph.D.
Professor in charge of thesis on behalf of the Advisory Committee

Approved: _____
Jack Gelb Jr., Ph.D.
Chair of the Department of Animal and Food Sciences

Approved: _____
Mark Rieger, Ph.D.
Dean of the College of Agriculture and Natural Resources

Approved: _____
James G. Richards, Ph.D.
Vice Provost for Graduate and Professional Education

ACKNOWLEDGMENTS

Carl Schmidt, Ph.D. for his continuous advice, guidance, and academic support during the past several years.

My fellow students and colleagues who have supported and helped me throughout my graduate education.

This manuscript is dedicated to:

My husband, Eric Enslen, for his love, patience, and understanding. I could not have achieved this goal without his support and encouragement.

My family, for their unconditional love and support.

TABLE OF CONTENTS

LIST OF TABLES

LIST OF FIGURES

ABSTRACT

Modern broiler chickens have been selected for rapid growth and optimal feed efficiency. Comparing modern and heritage broiler lines provides insight into the changes that have occurred during human directed selection. Previous work comparing Ross708 and a Heritage line maintained at the University of Illinois revealed significant differences in normalized organ sizes at different age points. In this study, we have analyzed morphometric data from birds of both lines and investigated gene expression patterns in tissue samples from the liver, heart, breast muscle, duodenum, and cerebellum. Comparing gene expression levels between the tissues provides insight into the relative complexity of each, with heart, duodenum, and brain samples displaying the largest amount of unique gene expression. Additionally, the relationship between qPCR experiments and RPKM values obtained from ERANGE is explored to assess their relative accuracy and establish a correlation between the two measurements of gene expression.

Chapter 1

INTRODUCTION

Since the domestication of the red junglefowl (*Gallus gallus gallus*) (Fumihito et al., 2006; Kanginakudru et al., 2008) around 7,000 to 10,000 years ago in Asia (Komiyama et al., 2004), the chicken has played an important role in human agriculture. Though first used for egg production, the modern market has seen tremendous growth in demand for chicken meat. As a result, chickens began to be selected for their meat production (broiler) traits. Selection for feed efficiency and growth rate greatly increased the productivity of the broiler industry, reducing the time needed to reach marketable weight from 16 weeks to 6-7 weeks in just 40 years (Thomas et al., 1958; Warren, 1958; Griffin and Goddard, 1994; Konarzewski et al., 2000).

This selection for rapid growth has had effects on many of the major organ systems. Changes have been observed in the muscle, digestive, nervous, cardiovascular, integumentary, and immune systems. The modern broiler has an insatiable appetite along with a greater efficiency for converting feed into body mass (Griffin and Goddard, 1994). One consequence of the stress of such rapid growth is the rise of cardiovascular failure (Olkowski et al., 2008), ascites (Morris, 1992), impaired immune function (Cheema et al., 2003), poor reproductive performance

(Reddy and Siegel, 1976; Hocking, 1993), and skeletal issues (Lilburn, 1994; Rath et al., 2000; McDevitt et al., 2006).

The emergence of these various health-related problems allows for the evaluation of the consequences of human-directed evolution. Studying the effects of selection for rapid growth on organ systems can improve our understanding of their physiological interactions as well as relative resource allocation between different organ systems. Furthermore, understanding these system-wide interactions may aid in the improvements of breeding populations of broilers to further increase the production and health of these birds.

Previously, we have studied the morphological changes between strains of broiler chickens to understand the adaptations that have taken place in response to the selective pressures for rapid growth and feed efficiency (Schmidt et al., 2009). The present study expands the investigation into the morphological changes observed and seeks to characterize the chicken transcriptome and its adaptations to these selective pressures. The transcriptome of a species is the total set of all RNA produced by the organism's cells.

Like the previous study, this project uses a heritage broiler line (UIUC, developed by H. M. Scott and maintained at the University of Illinois Urbana campus) that has not been selected for rapid growth to serve as a baseline for characterization of changes over time (Schoettle et al., 1956a,b; Waterhouse and Scott, 1962). The heritage birds are the progeny of males from a New Hampshire line crossed with females carrying the Columbian feather pattern to allow feather sexing (Schmidt et al.,

2009). The New Hampshire line used to generate the males has been inbred since the late 1940s. The Columbian female line was originally derived from a cross between Barred and White Plymouth Rocks and has also been inbred since the late 1940s. The commercial line (Ross 708) is grown under the same conditions as the heritage line in order to allow morphological and genetic comparisons.

Our hypothesis is that changes in gene expression have played a role in the responses that we have observed in intense selection for growth. The chicken transcriptome has not yet been deeply characterized at a global and tissue-specific-level. Unlike the genome, the transcriptome is extremely flexible and sensitive to environmental stimuli, allowing for the study of differential gene expression under various conditions. Since the transcriptome includes all of the mRNA transcripts in the sample, it reflects which genes are being expressed in the sample tissue at that moment and it provides a glimpse into the processes ongoing in particular sets of cells.

A recent study of the human transcriptome by Ramsköld, Wang, Burge, and Sandberg (2009) revealed a large number of ubiquitously-expressed genes shared amongst the various tissues of the human body. Gene products which were relatively unique or tissue-specific tended to be found within the plasma membrane or secreted into the extracellular environment, whereas those found in most or all tissues tended to be intracellular and involved in core cell functions (Ramsköld, et al., 2009). They noted high correlations between orthologous gene expression in humans and mice, but did not investigate chicken gene expression.

The objective of this study was to determine the differences between the two chicken lines (Ross and Heritage) in terms of quantitative physical traits and to provide a tissue by tissue analysis of the chicken transcriptome. The physical data is analyzed both as morphometric data (comparing the actual sizes of tissues and whole body mass) and allometric data, which uses a logarithmic transformation of the base values to compare relative growth. This study also sought to establish RNASeq reads in the form of reads per kilobase per million (RPKM) as a comparably reliable alternative to qRT-PCR by directly comparing the two using a control set of genes for detection.

Chapter 2

METHODOLOGY

2.1 General Experiment Overview

Heritage chicken line eggs were obtained from Chet Utterback of the University of Illinois, and Ross 708 eggs were obtained from Mountaire Farms in Millsboro, Delaware. The eggs (300 from each line) were incubated at 37°C until hatching.

Once hatched, females were removed from the flock to mimic industry procedure, simplify the experimental design and reduce gender effects. The chicks were placed in two large colony houses that were divided to permit housing of equivalent numbers of control and heat conditioned Heritage and Ross708 chicks. The chicks were placed in houses prewarmed to 33°C with the temperature reduced by 3°C each week until 21 days post-hatch (dph). At 21 dph, the temperature of the house was maintained at 24 °C for the following three weeks.

On days 7, 14, 21, and 42 post-hatch, birds were randomly selected from each house/breed combination, weighed and euthanized via cervical dislocation. Organs of interest were removed, weighed, and measured, including the entire small intestine (duodenum, jejunum, ileum), the heart, liver, the left half of the breast muscle (pectoralis major, doubled to determine total breast mass of each bird), spleen, and

brain (entire brain weighed, cerebellum collected). Small sections of each organ were collected and immediately frozen in liquid nitrogen. Samples were then stored at -80°C to maintain RNA integrity until they were processed.

2.2 RNA Isolation and Purification

Total RNA was purified from frozen tissue samples using the QIAGEN RNeasy Mini-Kit and Fibrous Tissue Mini-Kit when necessary. Frozen tissue was disrupted in a buffer (Buffer RLT) containing a high concentration of guanidine isothiocycanate and homogenized. Ethanol was then added to the lysate, promoting selective binding of RNA to the silica membrane of the spin columns provided in the kit. The sample was then washed with other washing buffers (RW1 and RPE) containing guanidine salt and ethanol to remove traces of salts and biomolecules that are non-specifically bound to the silica membrane while leaving RNA molecules larger than 200 bases bound to the column. After several washes, the RNA is eluted using RNAse-free water and its concentration determined using a Nanodrop spectrophotometer. RNA was checked for quality using the Agilent BioAnalyzer RNA chip (Agilent Technologies, Inc., Santa Clara, CA).

2.3 Transcriptome Library Generation

Transcriptome library synthesis was performed using the Illumina TruSeq RNA Sample Prep Kit following the manufacturer's protocol. The poly-A containing mRNA molecules isolated above were purified using poly-T oligo-attached magnetic

beads. Following purification, the mRNA was fragmented using divalent cations under elevated temperature. These RNA fragments were then copied into first strand cDNA using reverse transcriptase and random primers. A second strand of cDNA was then synthesized using DNA Polymerase I and RNase H. The ends of the cDNA fragments were repaired with the addition of a single adenine base and ligation of the adapters. The products were then purified and enriched with PCR to create the final cDNA library. The resulting libraries were then sequenced at the Delaware Biotechnology Institute Core Sequencing Facility. Transcription levels were determined using ERANGE software[1] and uploaded to the Bigbird Database[2].

2.4 Quantitative RT-PCR

First strand synthesis was done with superscript II Reverse Transcriptase (Life Technologies) according to the manufacturer's directions. qRT-PCR was done use gene specific primers and the Fast SYBER green master mix (Applied Biosystems) on an Applied Biosystems 7500 Fast Real Time PCR System according to the manufactures directions. Relative quantification was determined using the ΔΔCt method using HNRNPAB for normalization with fold changes calculated as $2^{-\Delta\Delta Ct}$.

---

[1] http://woldlab.caltech.edu/rnaseq

[2] http://bigbird.anr.udel.edu/tkeeler/bigbird_db/index.php

2.5 Statistical Analysis and Gene Ontology

RPKM data was retrieved from Bigbird and imported into JMP 10 Statistical Software (SAS Institute, Inc., Cary, NC) for analysis by various methods, including multivariate pairwise correlations, hierarchical clustering, and principal component analysis. Gene functions and related gene ontology (GO) terms for relevant gene lists were generated using the DAVID bioinformatics database[3] and the eGIFT database[4].

[3] http://david.abcc.ncifcrf.gov/

[4] http://biotm.cis.udel.edu/eGIFT/index.php

Chapter 3

MORPHOMETRIC AND ALLOMETRIC ANALYSIS

3.1 Overview

Morphometric data that was collected is presented in two formats: raw normalizations of organ mass (the organ mass divided by total body mass) and allometric plots. Allometric plots use a log scale to linearize relative relationships between body and tissue sizes. Differences in the slope and intercept indicate differences in proportion of trait size between the two groups.

3.2 Breast Muscle

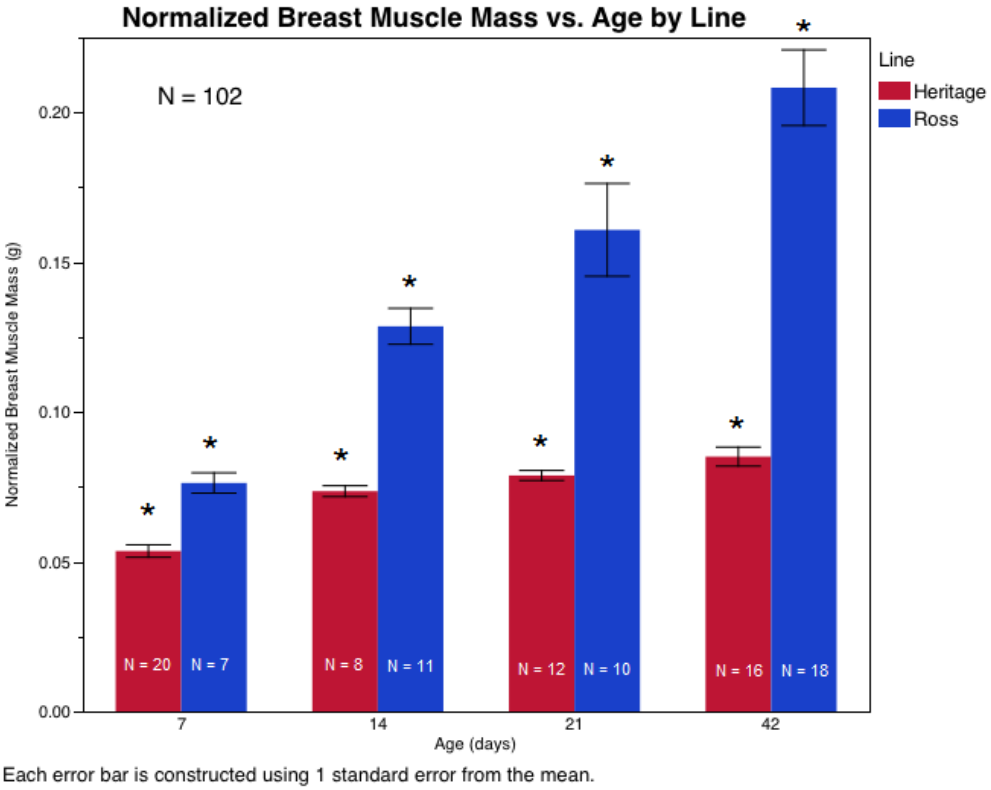

Figure 3.1: Average normalized breast muscle mass for each age group, separated by breed. Each error bar is constructed using 1 standard error from the mean.

The breast muscle mass of the Ross birds exceeded that of the corresponding Heritage birds at each age point (Figure 3.1). Ross birds were specifically bred for high growth and feed efficiency, allowing them to generate significantly more muscle tissue in a shorter time span. The Heritage birds maintain an approximately even ratio of breast muscle to body mass from about day 14 onward.

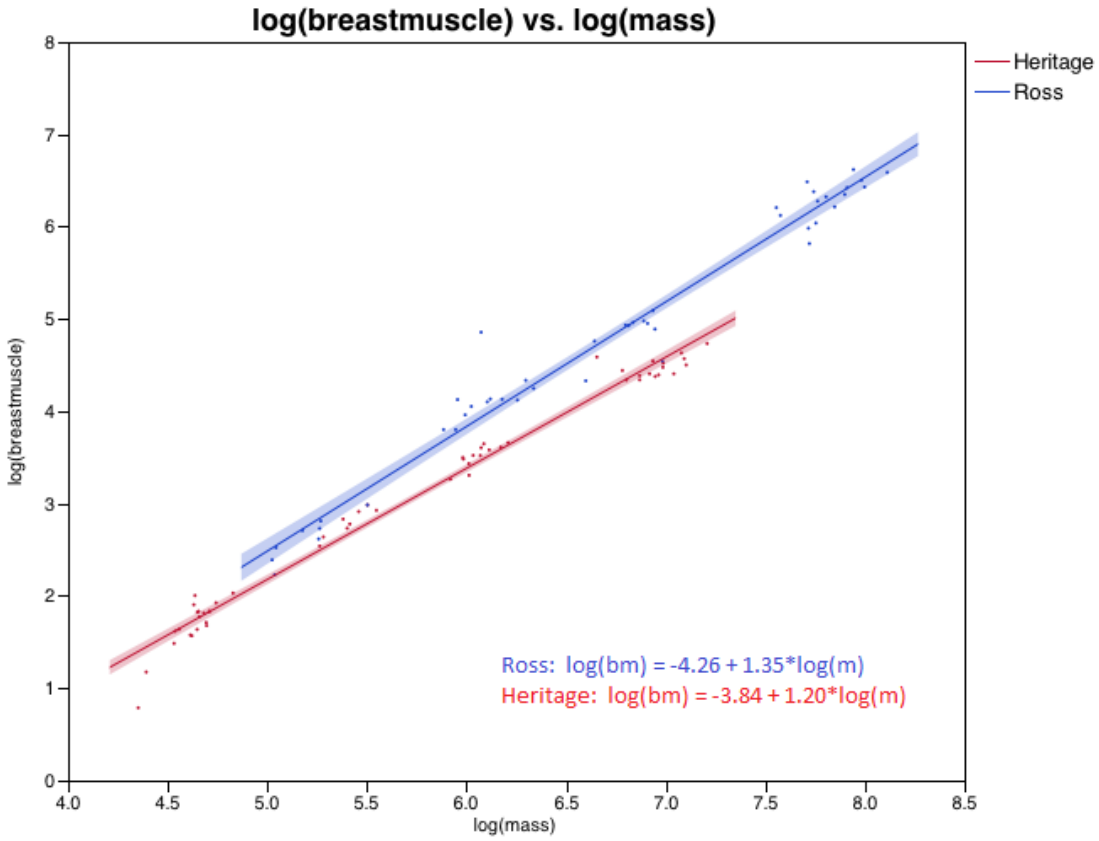

Figure 3.2: Allometric plot for breast muscle vs. total mass. The Ross birds have a much steeper slope relative to the Heritage birds.

The allometric plot confirms the increased growth rate of Ross breast muscles relative to those of their Heritage counterparts. Though the difference is difficult to see in Figure 3.2, a slight change in the slope leads to the dramatic differential growth seen in Figure 3.1.

3.3 Brain

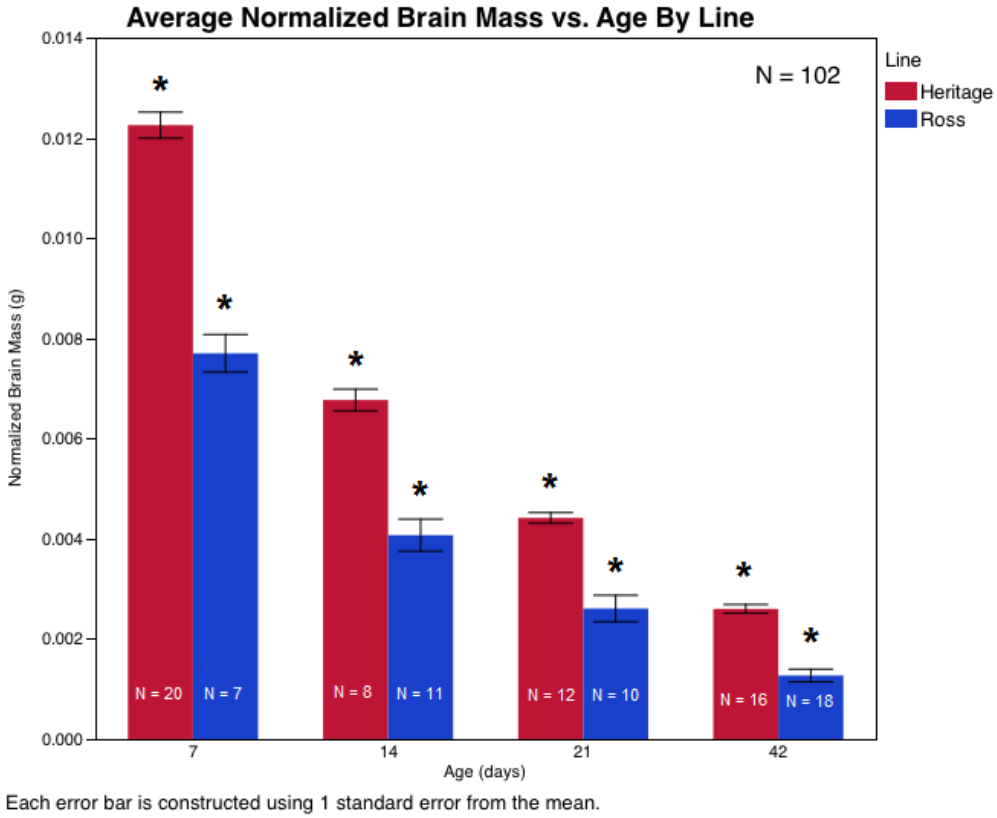

Figure 3.3: Average normalized brain mass for each age group, separated by breed. Each error bar is constructed using 1 standard error from the mean.

Normalization of brain mass to total body mass revealed a consistent trend between the two breeds. Heritage birds had proportionally larger brains at each age than their Ross counterparts (Figure 3.3). Development and maintenance of the brain requires significant energy resources. Possibly, selection for increased muscle mass has resulted in depriving the brain of nutrients. The Heritage birds at day 42 also exhibited a larger variance in brain proportions than that of the Ross. This pattern also

appeared at days 7 and 14 to a lesser degree, and the Heritage variability was lower than the Ross at day 21.

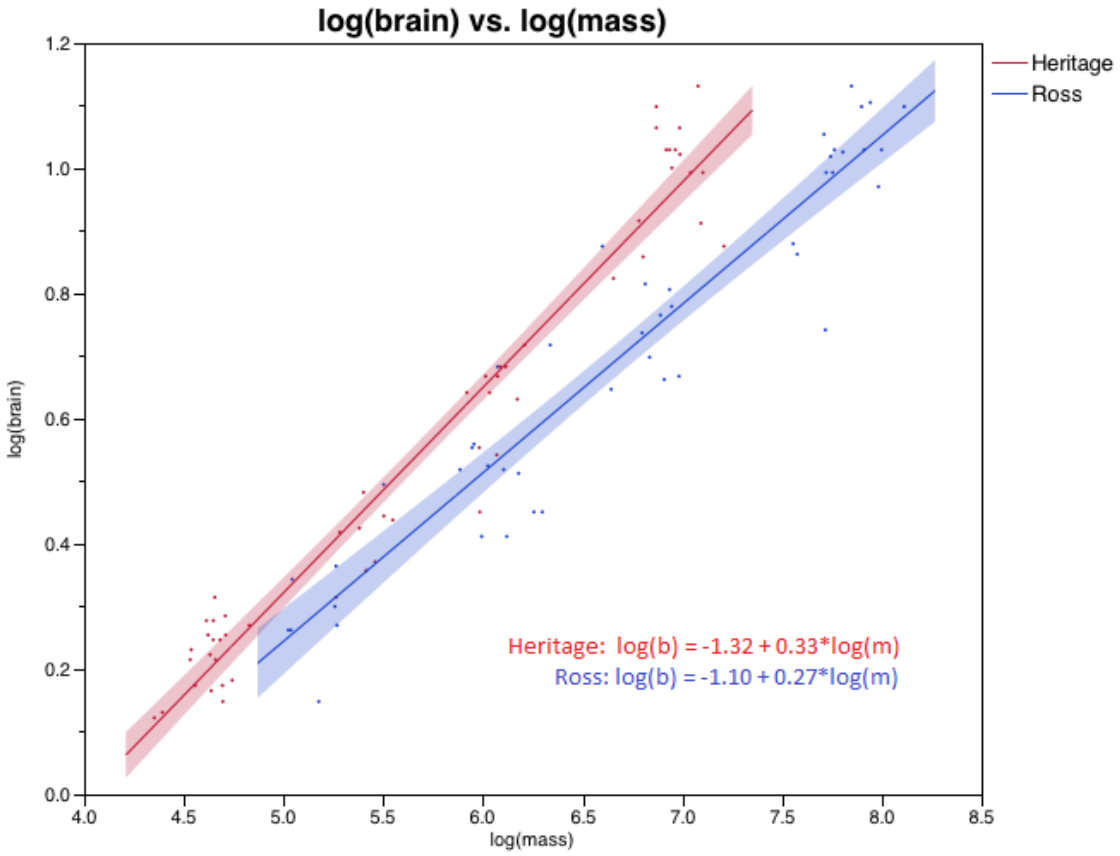

Figure 3.4: Allometric plot of brain mass vs. total mass. The Heritage birds display a much steeper slope relative to the Ross birds.

The allometric plot of the brain data confirms that the Heritage birds tended to have larger brains at a given mass. The slope of the linear relationship is higher in the Heritage than the Ross, indicating that brain size increases more per unit of total mass increase in the Heritage birds than in the Ross.

3.4 Heart

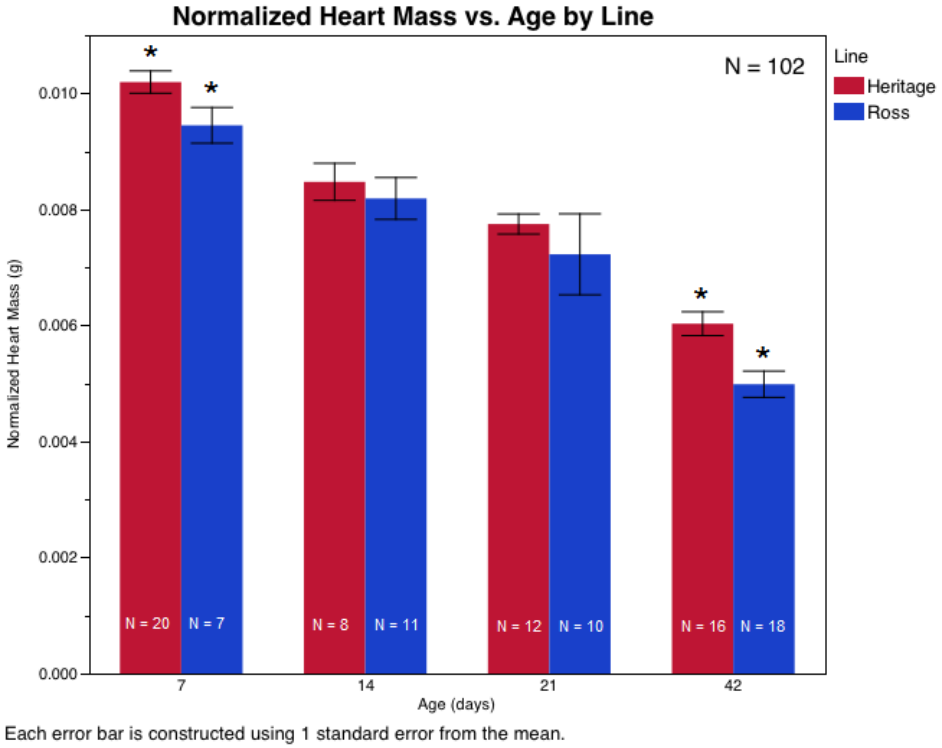

Figure 3.5 Average normalized heart mass for each age group, separated by breed. Each error bar is constructed using 1 standard error from the mean.

The Ross 708 line consistently displayed a lower average normalized heart size relative to that of the Heritage line, though the difference was only significant at days 7 and 42 (Figure 3.5). Possibly, the Ross birds are allocating more of their nutrition to production of skeletal muscle mass at the expense of cardiac tissue. Considering the size of the Ross birds, smaller hearts and decreased blood flow could pose significant health risks by overtasking the heart.

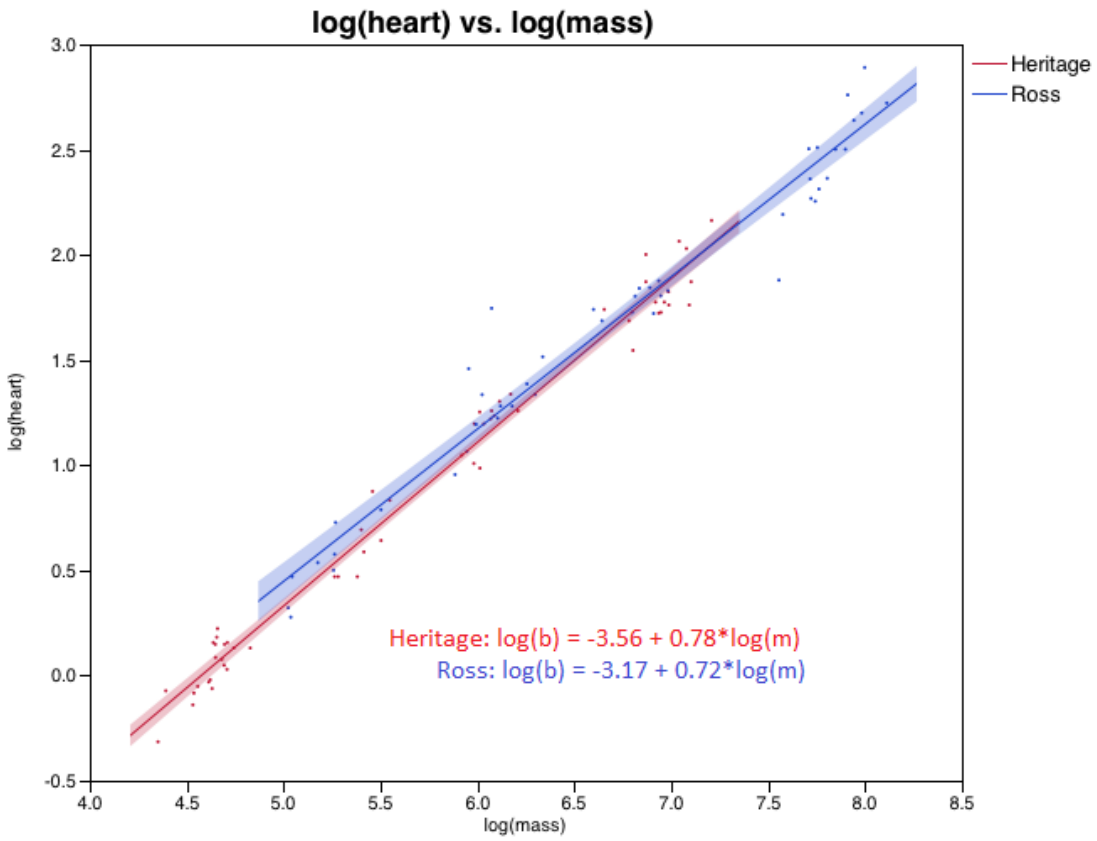

Figure 3.6: Allometric plot for heart mass vs. total mass.

The allometric relationship of the heart is interesting, since the slopes differ yet the data points themselves have considerable overlap. The overlapping data suggests that the heart does not have a significantly different relative growth between the two lines, which is a deviation from the findings reported in Schmidt et al., 2009. It is possible that the difference in housing between the two studies had an effect on the heart sizes. In the original study, the birds were kept in cages for the duration of the experiment which may have limited their movement and prevented them from

developing normally. In this study, the birds were in small colony houses and they had fewer restrictions on their movement.

3.5 Liver

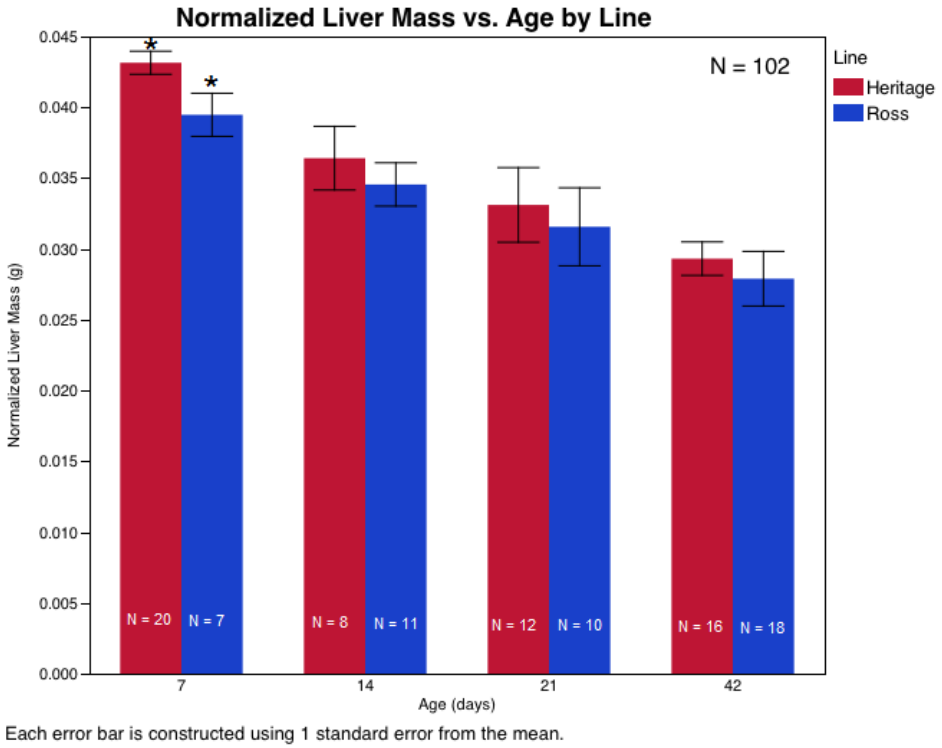

Figure 3.7: Average normalized liver mass for each age group, separated by breed. Each error bar is constructed using 1 standard error from the mean.

Normalized liver mass trended similarly to that of the heart, with the Ross birds displaying significantly smaller average liver sizes at day 7, but not significantly thereafter (Figure 3.7).

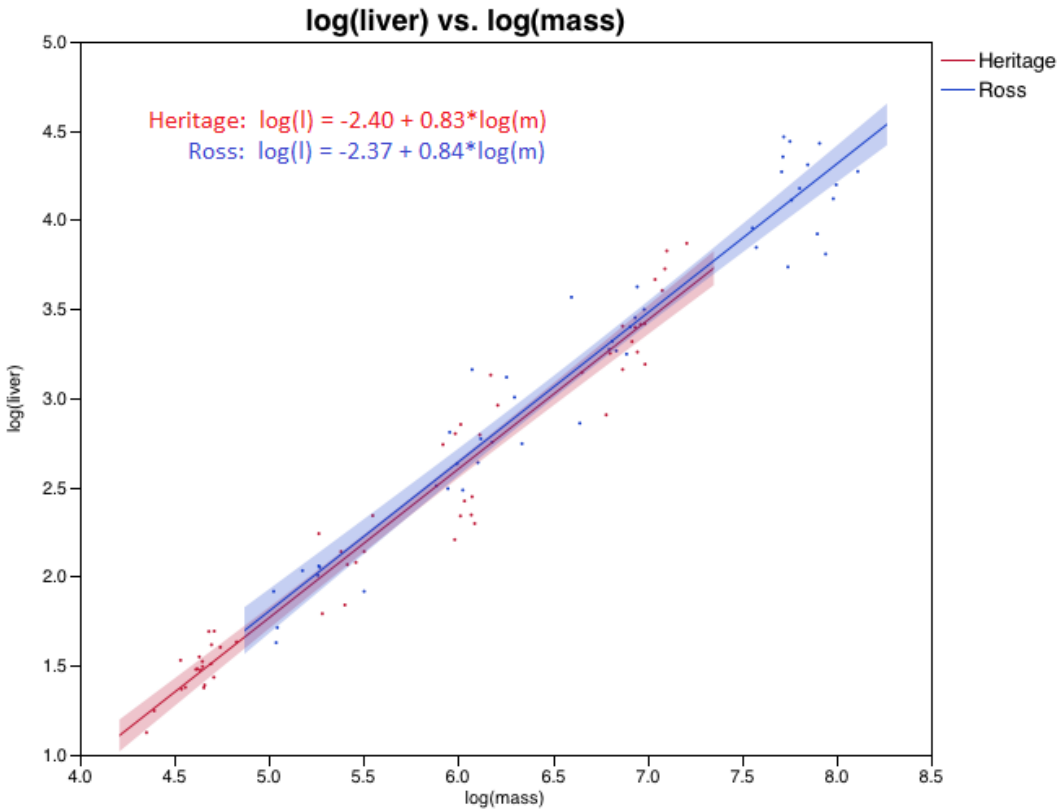

Figure 3.8: Allometric plot of liver mass vs. total mass. The two equations are extraordinarily similar.

Allometric data for the liver suggests that there is no significant difference in the relative scaling of the liver between the two lines. The equations of the lines of best fit are identical and the plot shows both are superimposable.

3.6 Spleen

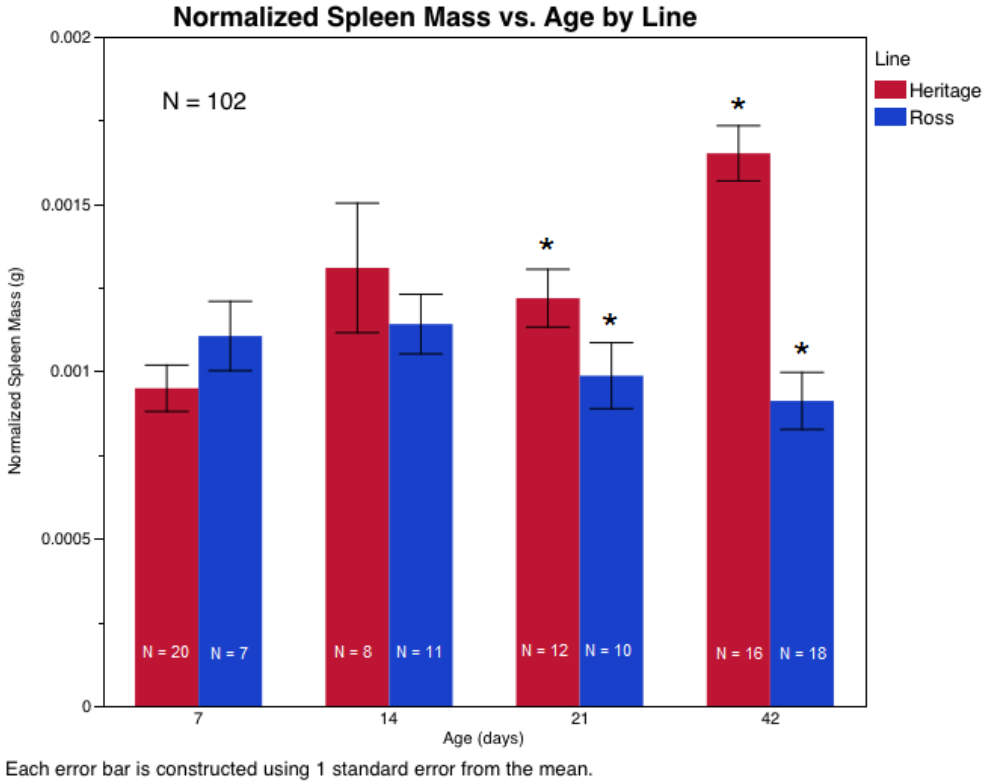

Figure 3.9: Average normalized spleen mass for each age group, separated by breed. Each error bar is constructed using 1 standard error from the mean.

At days 7 and 14, the spleens of both lines were not significantly different, but the Heritage became significantly larger at days 21 and 42 (Figure 3.9) relative to body weight. Given the important role of the spleen in immune function, this could suggest that the Ross birds have allocated significant amounts of nutrients to production of muscle mass at the expense of the immune system, potentially leaving them more vulnerable to disease than their Heritage counterparts. Additionally, a smaller spleen size reduces the potential amount of erythrocyte storage and limits erythrocyte filtering and replenishment.

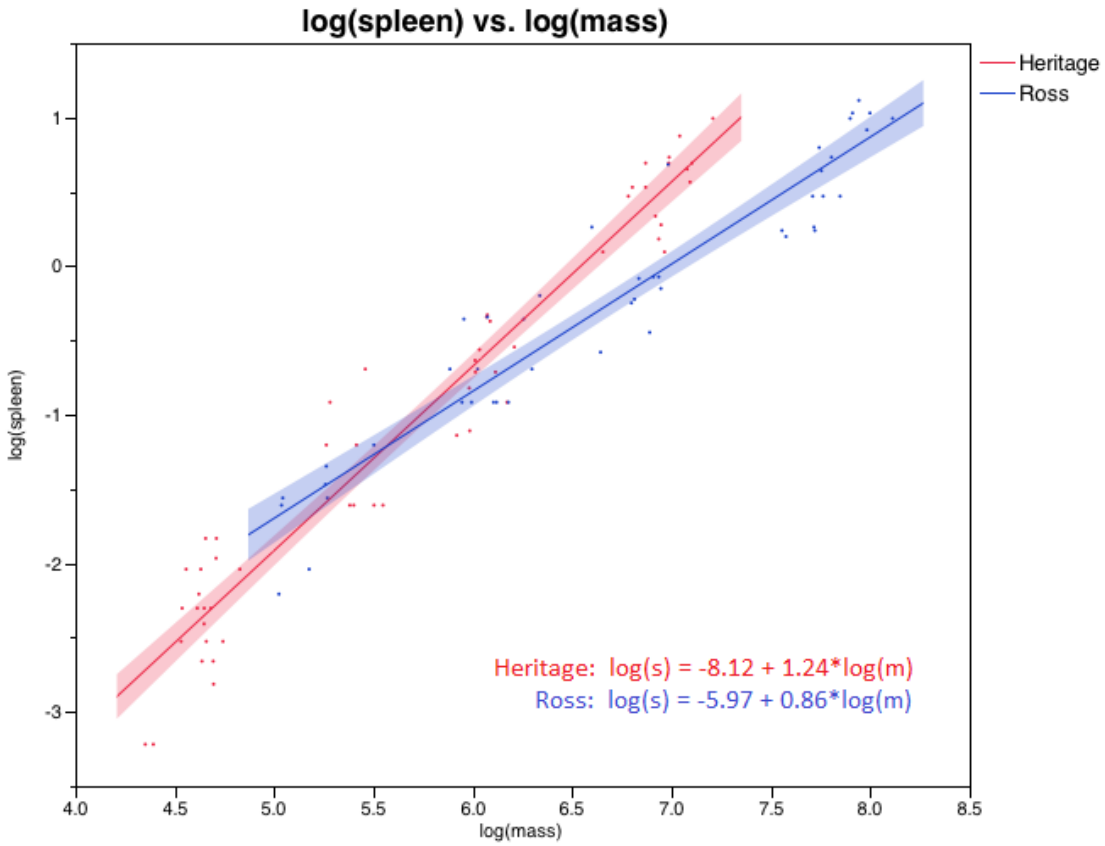

Figure 3.10: Allometric plot of spleen mass vs. total mass. There is a drastic difference in slope between the two groups.

The allometric relationships support the contention that the Heritage spleens grow at a faster rate relative to their body than the Ross counterparts.

3.7 Small Intestine

Morphometric analysis of the segments of the small intestine yielded some interesting results. As one moves along the intestine, each segment becomes increasingly longer in the Ross birds, yet less massive. Heritage duodenums were

more massive at all age points and tended to be longer than Ross duodenums at similar body masses (Figures 3.11 and 3.12). In the jejunum, both lines were fairly similar in mass and there were no significant differences until day 42, at which time the Heritage birds had significantly more massive jejunums (Figure 3.13). When jejunum lengths are compared, however, Ross birds consistently had significantly longer jejunums than the Heritage line when compared at a similar body mass (Figure 3.14). Moving further to the ileum, the Ross birds have heavier ileum weights until day 42 (significantly larger at day 7 and 21, significantly smaller at 42; Figure 3.15). The ileum length trend follows that of the jejunum: the Ross line consistently had significantly longer ileum lengths at comparable body mass (Figure 3.16).

These findings about the intestinal tract are interesting given that the Ross line has undergone artificial selection for increased feed efficiency and growth. The smaller masses of the Ross intestinal segments are interesting, as one would expect the intestinal lining to be thicker and have longer villi to increase surface area for absorption, thereby increasing the mass relative to the Heritage intestinal segments. Given that these tissues are also longer, the revelation that they are actually lighter raises some interesting questions. The Ross line could possibly have decreased the overall size of the intestine to limit the size of the lumen rather than increasing the wall of the mucosa, effectively allowing for higher surface area by reducing the amount of ingesta allowed to flow through a given space at one time. Increasing the length of the intestinal tract supports this theory, since a longer intestine would allow more time for nutrient absorption while still allowing a thinner intestinal lining. In

this way, the Ross birds manage to absorb similar or greater amounts of nutrients while using less energy to maintain the intestinal structures due to their decreased mass. Histological analysis is needed to determine the validity of these hypotheses.

3.7.1 Duodenum

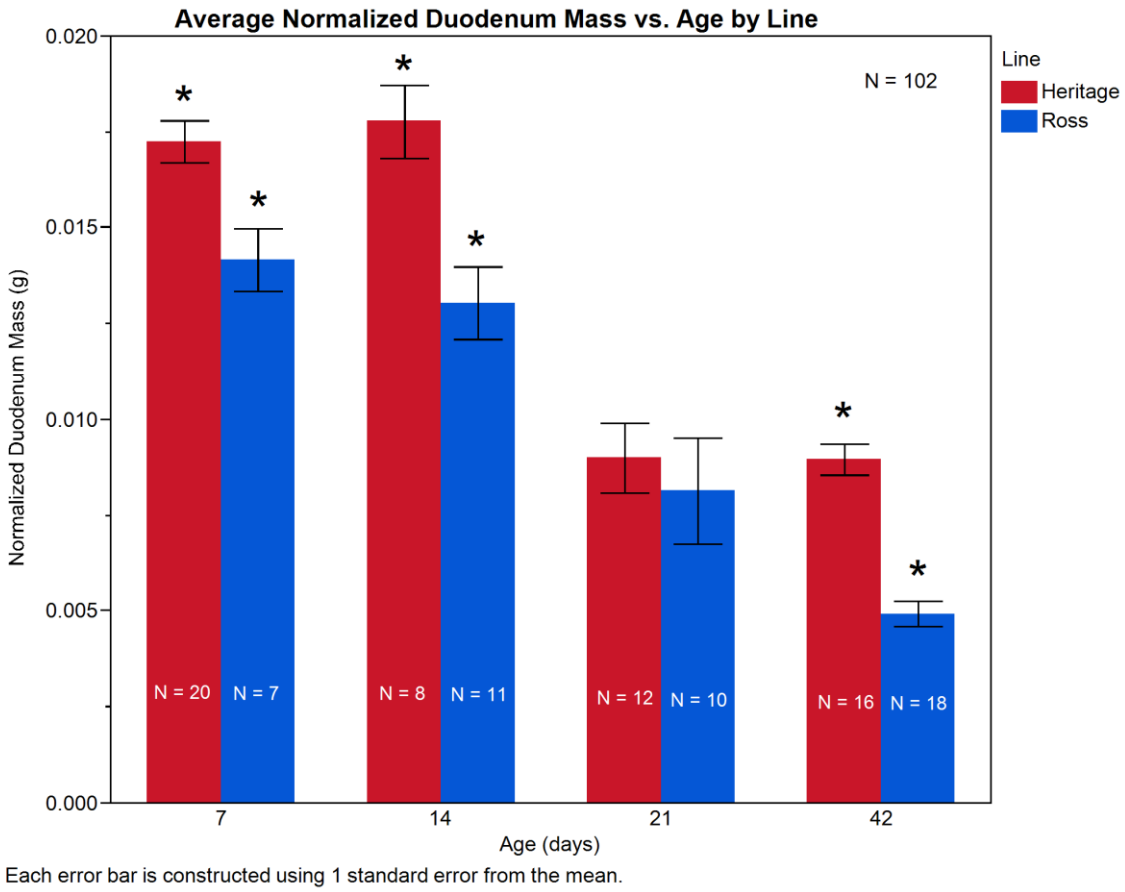

Figure 3.11: Average normalized duodenum mass for each age group, separated by breed. Each error bar is constructed using 1 standard error from the mean.

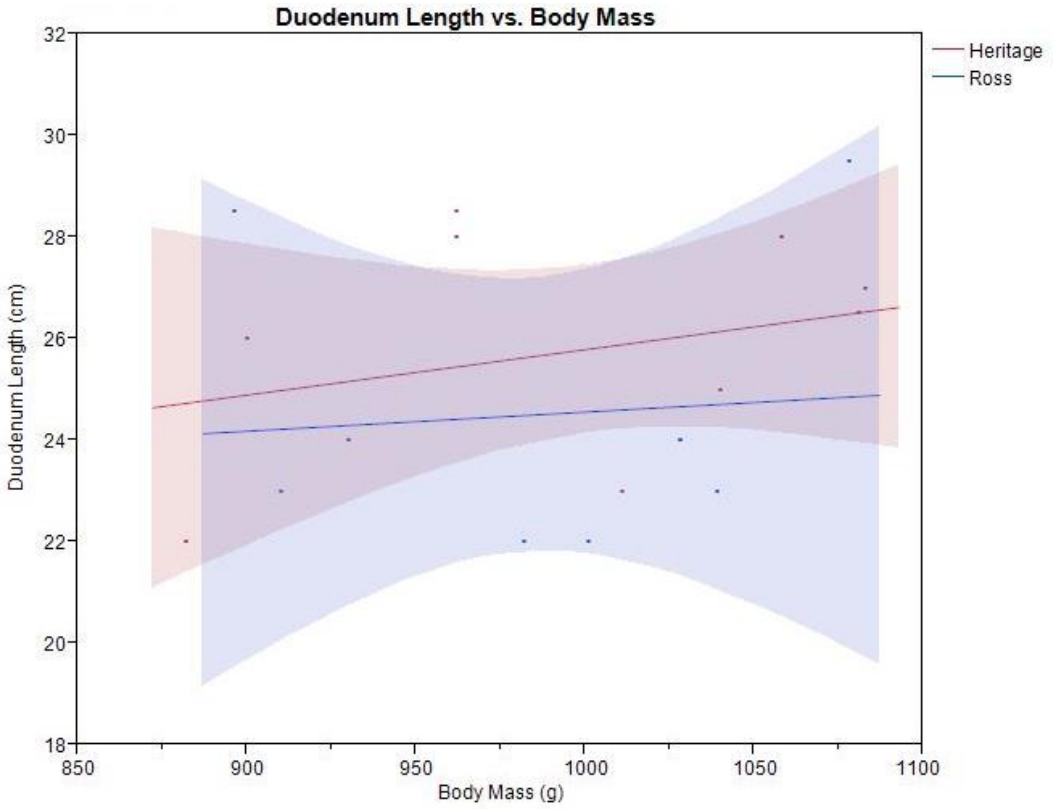

Figure 3.12: Average duodenum length (in centimeters) versus total bird mass (in grams), separated by line (Heritage in red, Ross in blue). Lines represent an approximate line of fit, dots represent actual data points. Ross: N=8, Heritage: N=10; data points chosen based on birds of comparable body mass.

3.7.2 Jejunum

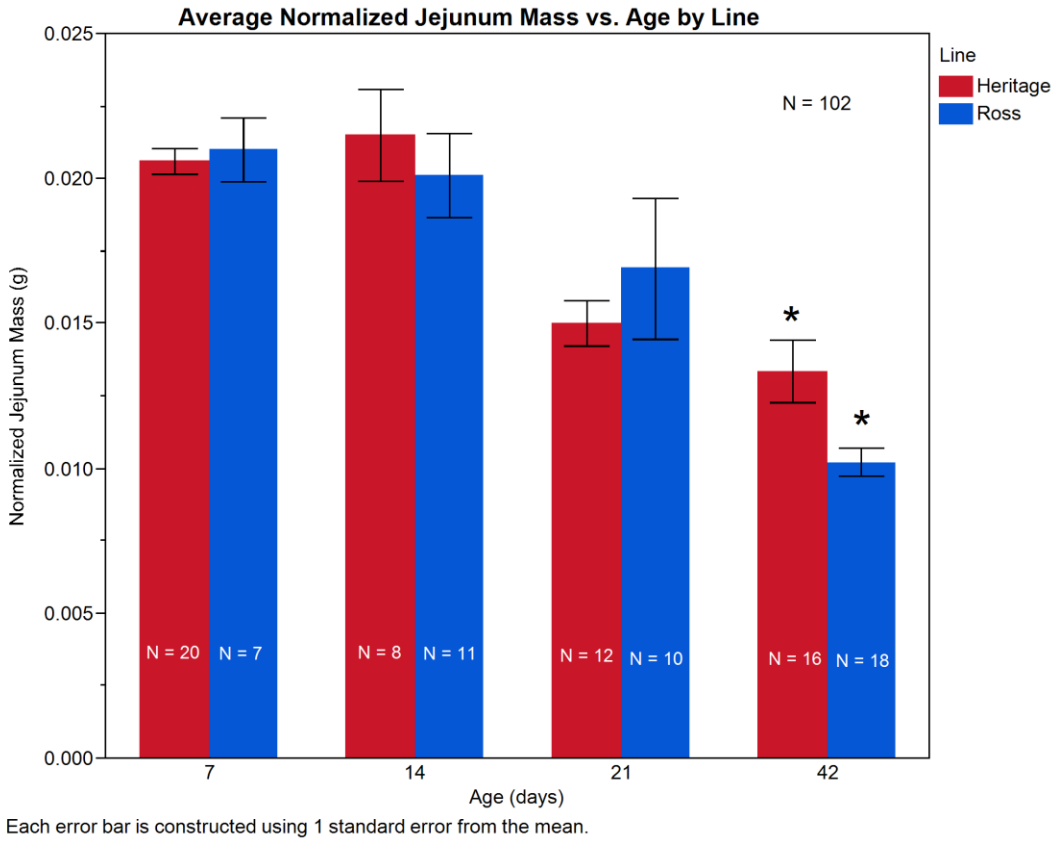

Figure 3.13: Average normalized jejunum mass for each age group, separated by breed. Each error bar is constructed using 1 standard error from the mean.

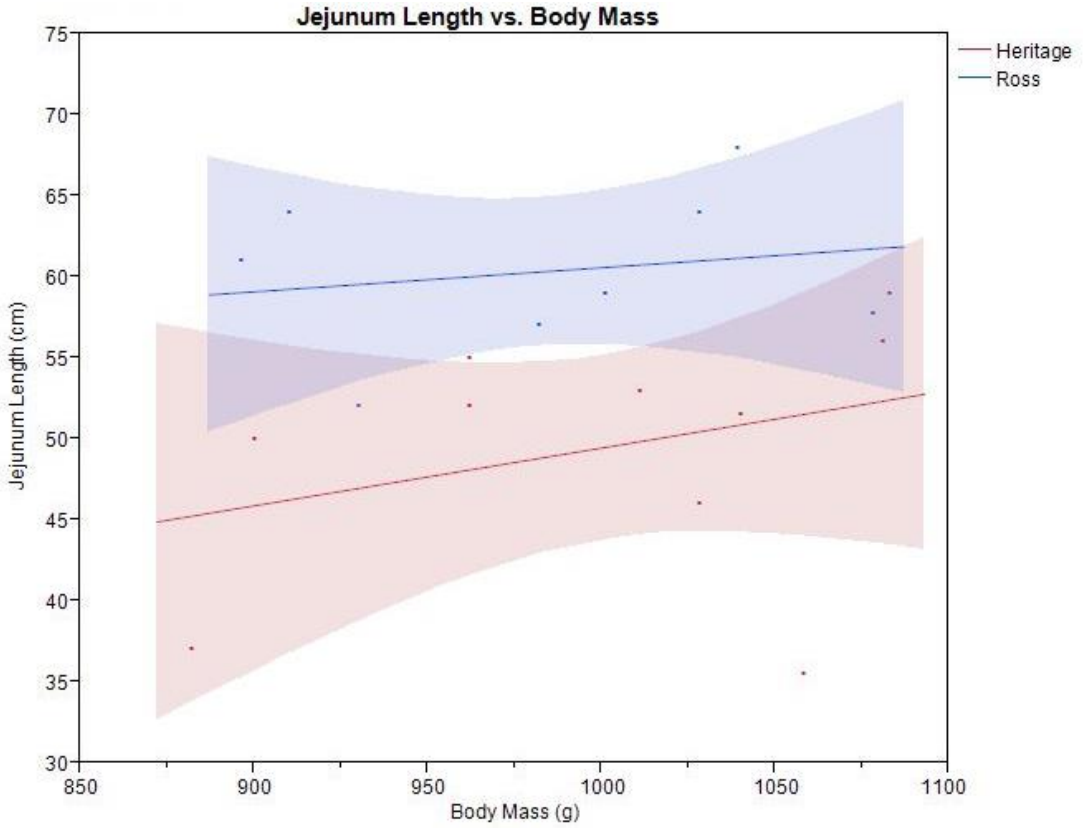

Figure 3.14: Average jejunum length (in centimeters) versus total bird mass (in grams), separated by line (Heritage in red, Ross in blue). Lines represent an approximate line of fit, dots represent actual data points. Ross: N=8, Heritage: N=10; data points chosen based on birds of comparable body mass.

3.7.3 Ileum

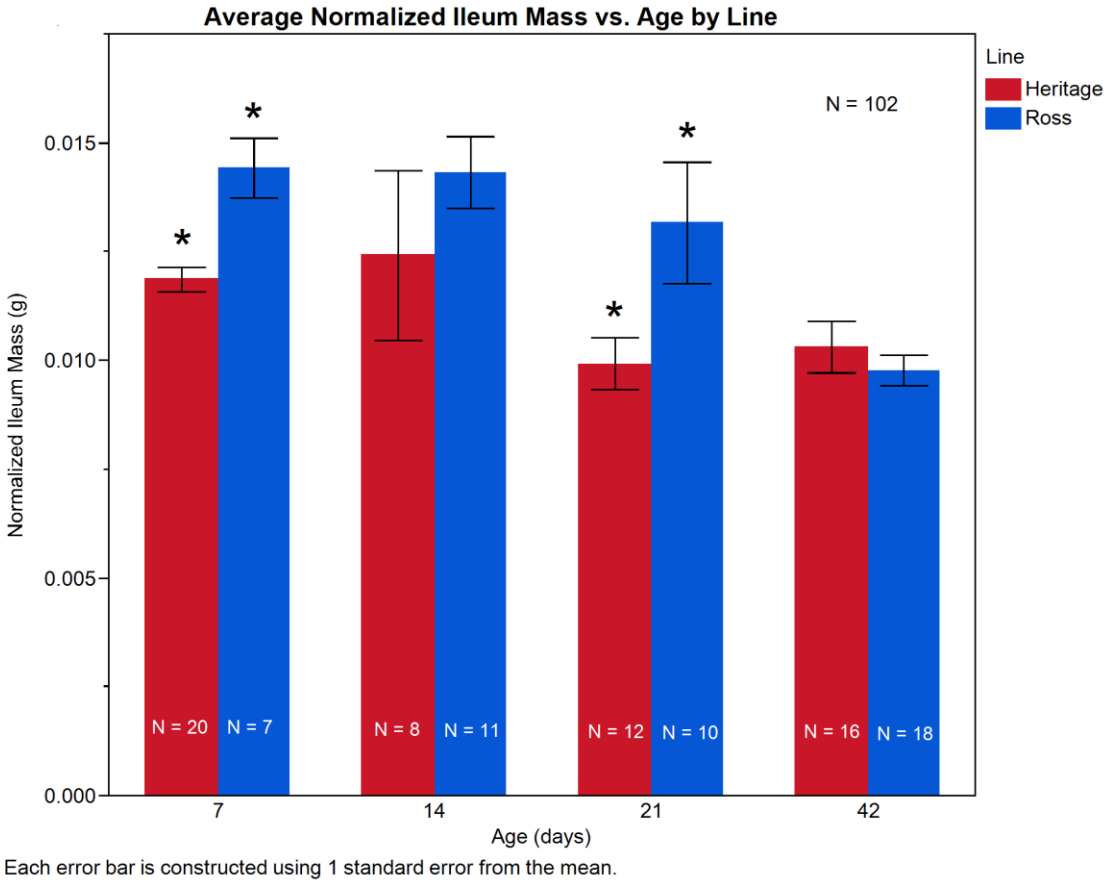

Figure 3.15: Average normalized ileum mass for each age group, separated by breed. Each error bar is constructed using 1 standard error from the mean.

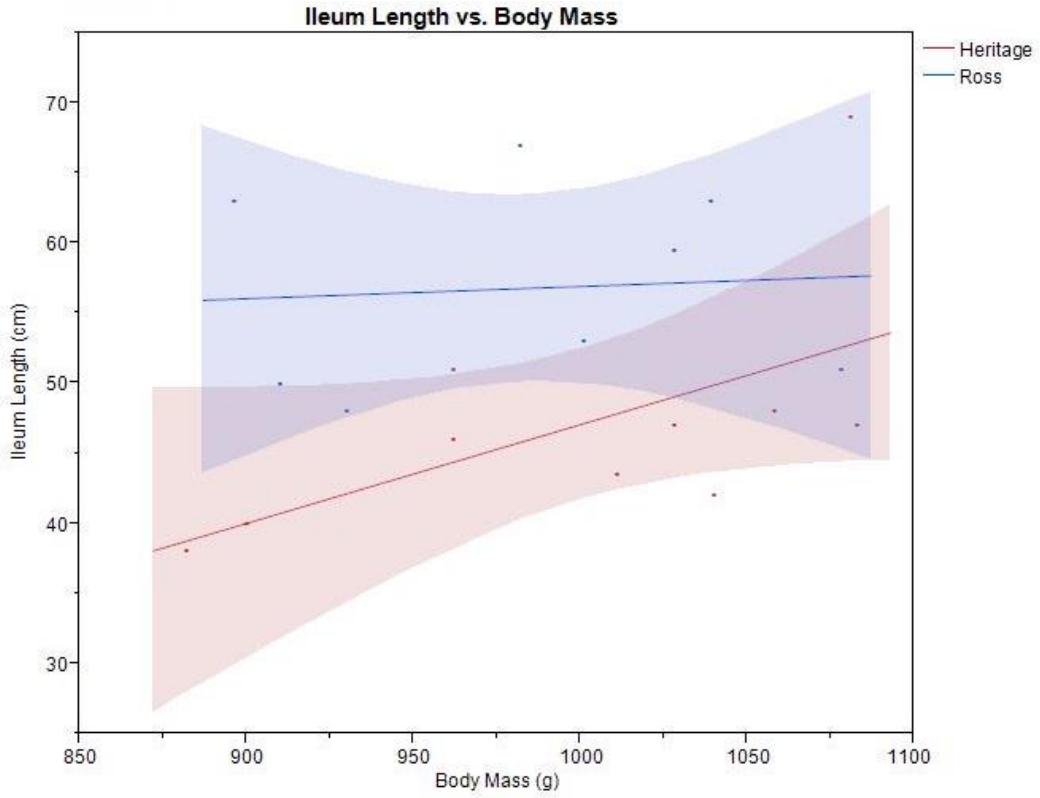

Figure 3.16: Average ileum length (in centimeters) versus total bird mass (in grams), separated by line (Heritage in red, Ross in blue). Lines represent an approximate line of fit, dots represent actual data points. Ross: N=8, Heritage: N=10; data points chosen based on birds of comparable body mass.

Chapter 4

RELATIONSHIP OF RNA-SEQ (RPKM) AND QRT-PCR (C_t)

In order to determine what cutoff values were appropriate for analyzing the RNA-Seq results, it was necessary to ascertain what range of RPKM values could be verified as accurate by another source. As real-time reverse-transcription polymerase chain reaction (qRT-PCR) has been highly regarded as an accurate method of detecting the amount of specific nucleotide sequences in a sample, it was the natural choice for comparison to RNA-Seq.

Using the gene expression RPKM values from samples obtained from RNA-Seq in cerebellar tissue, a set of 40 genes was chosen whose expression values were consistent across various samples and ranged from very low expression (0.08 RPKM) to high expression (724.16 RPKM). Each gene was detected in a previously-sequenced tissue sample via qRT-PCR and the resulting C_t values were compared to the log base 2 of the RPKM value already obtained from RNA-Seq. Detecting the same genes using both methods in an identical sample allows for determination of the correlation of accuracy between both procedures. In particular, using genes for which there were very high and very low expression levels detected in the given sample provides a range of values that can be used with confidence in statistical analysis.

Plotting the values against one another revealed a negative linear relationship (Figure 4.1) between C_t and Log_2RPKM and it indicated that RPKM values as low as 0.1 could be reliably detected by qRT-PCR. Based on these results, 0.1 was a cutoff value for expression in later analyses. A full table of genes used and subsequent RPKM and Ct values can be found in Appendix B.

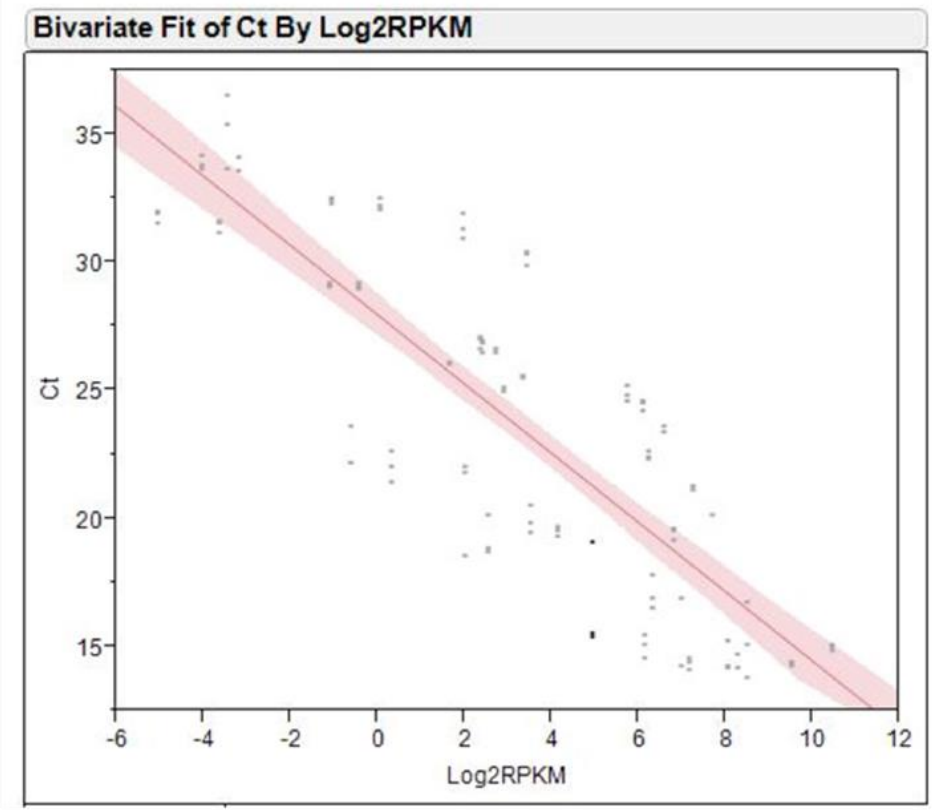

Figure 4.1: Plot of the C_t value from qPCR analysis versus the RPKM value from ERANGE for each gene. Genes displaying both high and low expression levels were randomly selected and plotted to determine a relationship between the two measures. The red line indicates a linear regression model with an R-square value of 0.71 and the red shading highlights the confidence interval.

Chapter 5

TRANSCRIPTOME ANALYSIS

5.1 Overview

Transcriptomes were generated for the liver, heart, breast muscle, duodenum, and cerebellum across different ages of both breeds. Genes were considered to be expressed if they were detected at a level of greater than or equal to 0.1 RPKM. Genes were further demarcated as consistent in a given tissue if the standard deviation of expression values across all samples was less than 20% of the mean expression value. Using these guidelines, 14,557 individual genes were detected in at least one of the tissues characterized. Of those, 5,540 genes were expressed at a consistent level in at least one of the tissues.

Tissue	# of consistently expressed genes	# of unique consistently expressed genes
Liver	70	15
Heart	2,409	928
Breast Muscle	784	140
Duodenum	2,771	1,822
Cerebellum	2,011	627

Table 5.1: Total number of genes expressed consistently in each tissue and the number of unique consistently expressed genes by tissue. The total number of consistently expressed genes across all tissues is 5,540; there is some overlap between gene expression in the tissues.

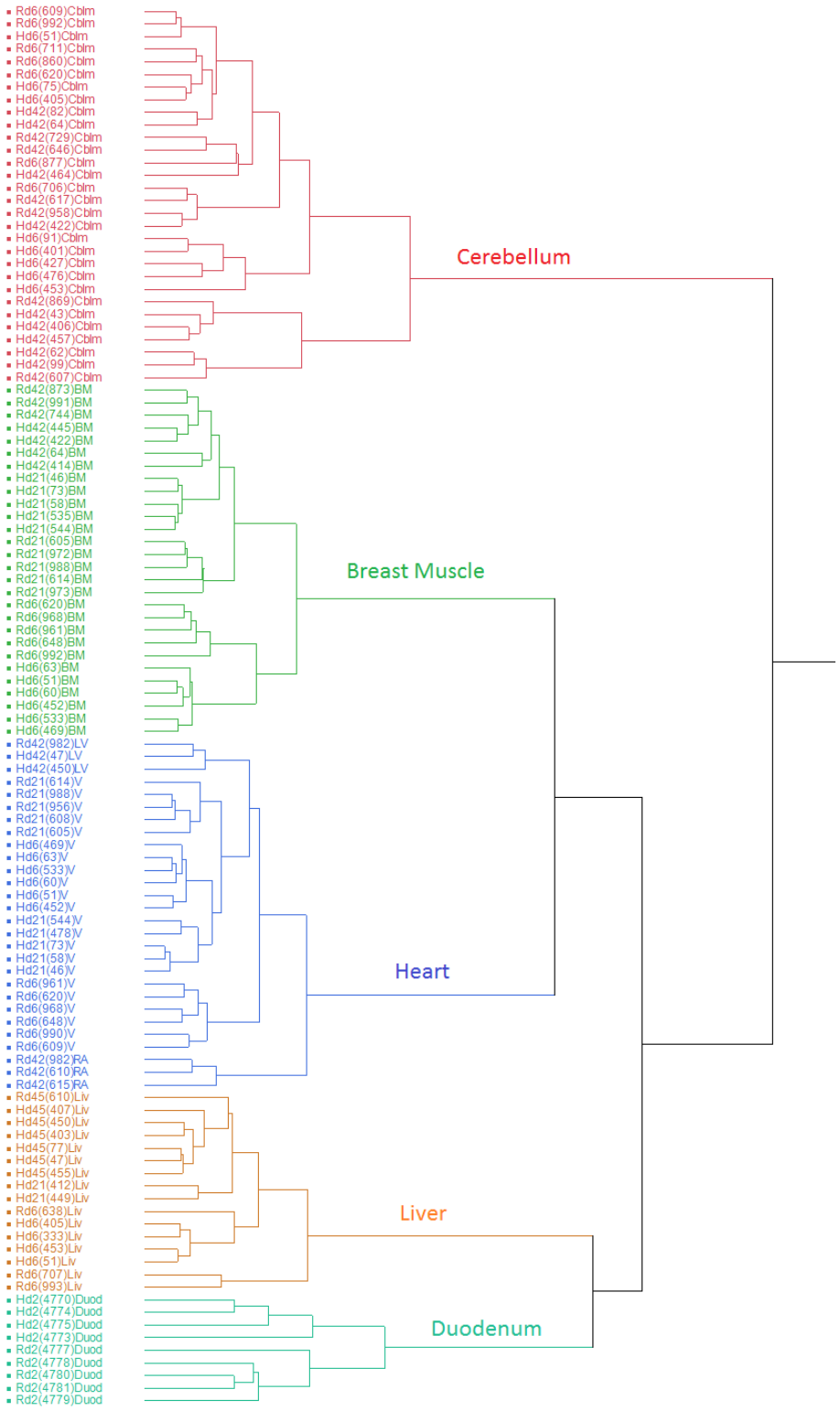

Figure 5.1: Hierarchical clustering of RNA-Seq reads from various tissues. Different tissue clusters have been assigned different colors for easier distinction.

Tissue transcriptomes were also compared to identify genes expressed across all tissues along with genes that appeared to be uniquely expressed in an individual tissue (Table 5.1).

Using JMP 10 Statistical Software, all RNA-Seq data from the various tissue samples were compared to one another in a cluster analysis to reveal potential genetic relationships between tissues. The resulting dendrogram (Figure 5.1) provided insight into the relative similarity between tissues. The cerebellum is the most distinct tissue, branching off first. The heart and breast muscle cluster together apart from the duodenum and liver. This is reasonable since both the heart and breast muscle are comprised mainly of muscular tissue. Heart tissue is further segregated into ventricular and atrial tissue, though samples of more atria are needed to confirm the clustering results. Despite structural differences between cardiac and skeletal muscle, the similarities between them were enough to separate them from the intestinal and liver samples.

5.2 Clustering within Tissues

5.2.1 Breast Muscle

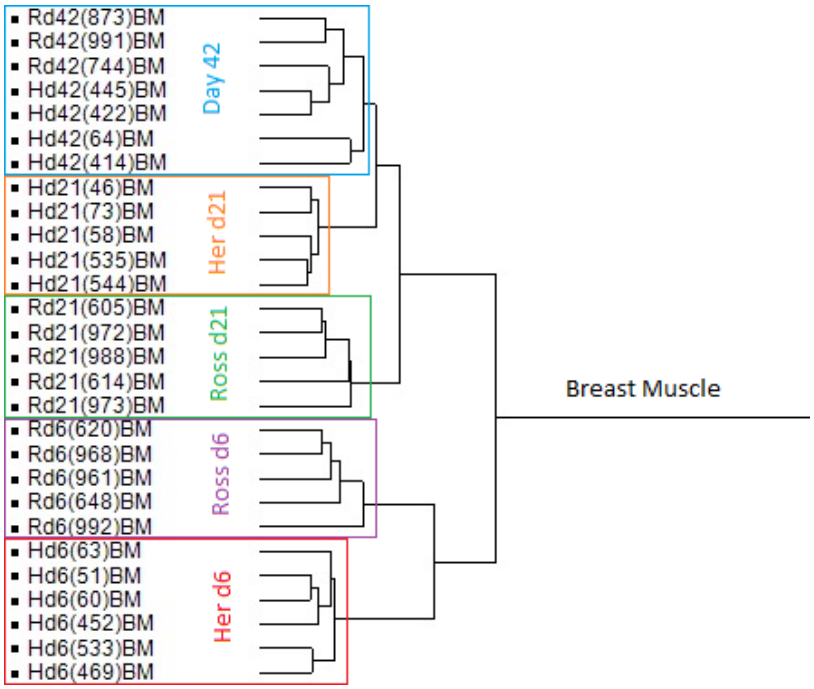

Figure 5.2: Hierarchical clustering of breast muscle samples. Colored boxes highlight the age and/or breed that characterizes the cluster.

5.2.2 Heart

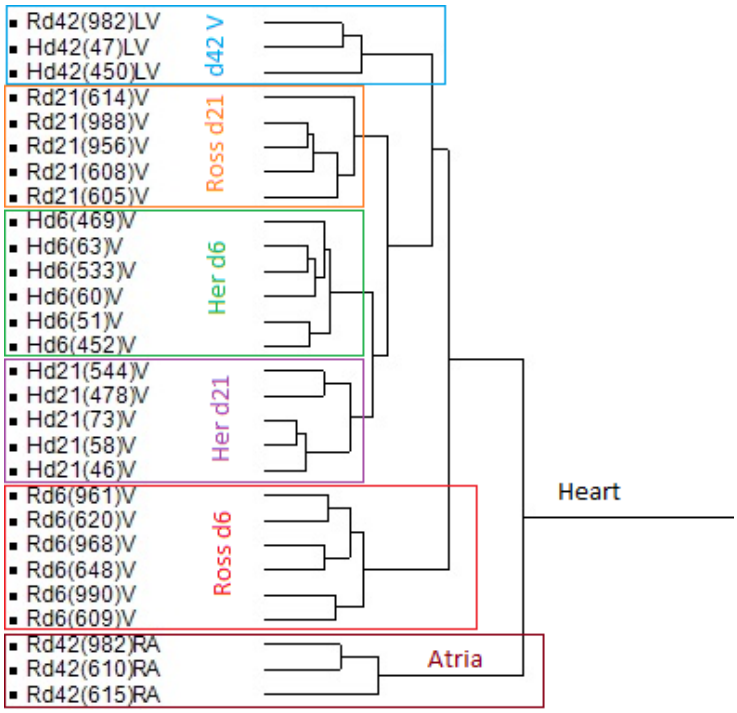

Figure 5.3: Hierarchical clustering of heart samples. Colored boxes highlight the age/or breed that characterizes the cluster, with the exception of the bottom brown box which highlights samples from the right atrium rather than the ventricle.

5.2.3 Liver

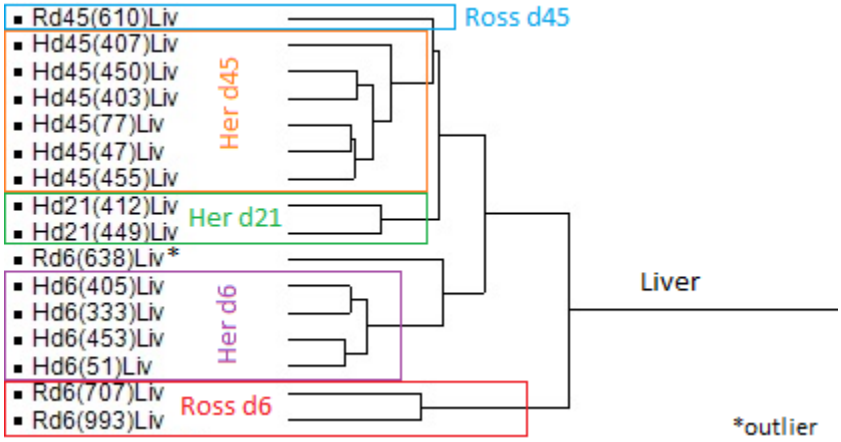

Figure 5.4: Hierarchical clustering of liver samples. Colored boxes highlight the age/breed that characterize the cluster. The (*) symbol denotes a sample that was unusual and did not cluster with the other samples of the same group.

5.2.4 Duodenum

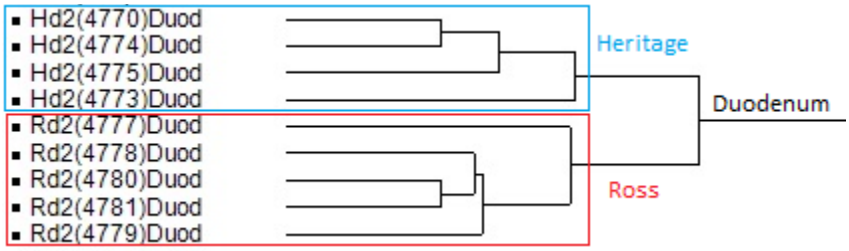

Figure 5.5: Hierarchical clustering of duodenum samples. Colored boxes highlight the breed characterizing each cluster.

5.3 Muscle Tissue

5.3.1 Breast Muscle vs. Other Tissues

Principle component analysis was performed on the entire population of samples to identify the genes that played a large role in driving the segregation of the tissues. The breast muscle samples separated dramatically from the other tissues, implicating a set of 10 genes (GAPDH, LDHA, MYL1, PGAM1, PGK1, PKM2, TNNI2, TNNT3, TPI1, and TPM1) that were upregulated in the breast muscle tissue. DAVID analysis revealed that the majority of these genes have functions related to glycolysis, pyruvate metabolism, and/or muscular contraction. The breast muscle had significantly greater expression of glycolytic pathway genes than even the heart, due to its dependence on glycolytic pathways for the majority of its energy compared to the heart's preference for fatty acid metabolism.

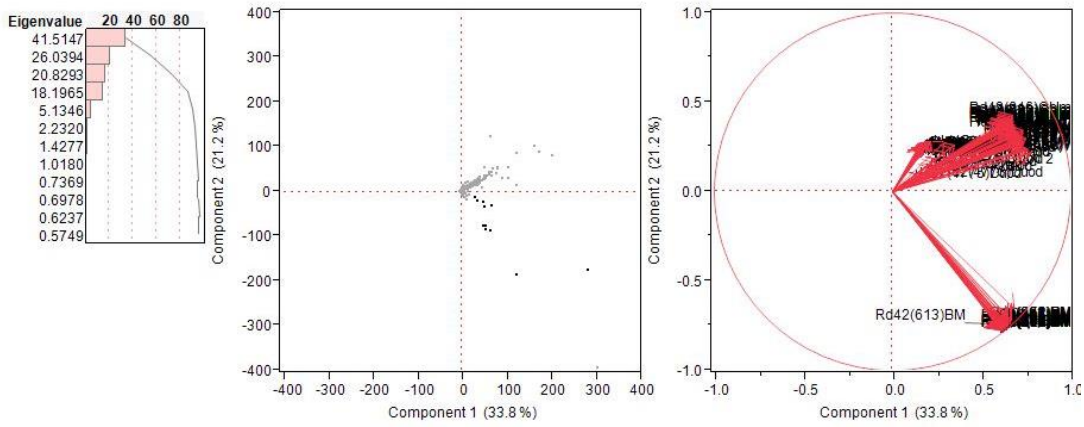

Figure 5.6: Principle component analysis of the correlation between gene expression values (RPKM) for all of the tissue samples, displaying the tendency of the breast muscle samples to diverge from the other tissues.

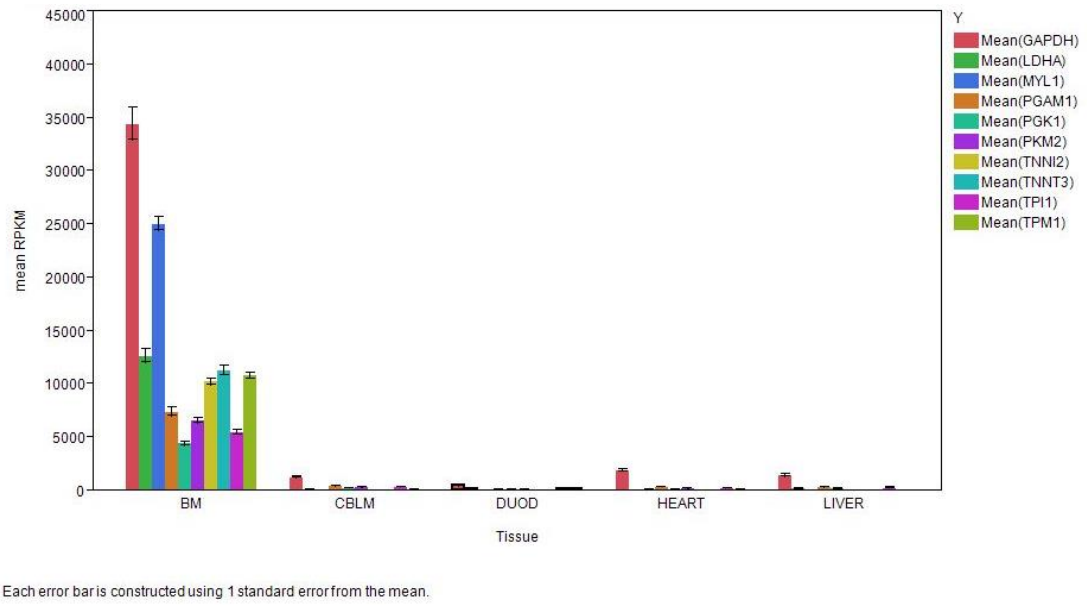

Figure 5.7: Comparison of expression levels of 10 genes discovered to be major factors in the separation of breast muscle from other tissues in principle component analysis.

5.3.2 Breast Muscle vs. Cardiac Muscle

Since the breast muscle and cardiac muscle clustered together in the dendrogram, the next step was to determine the major genes underlying the differences in the two muscle types. Following the same procedure as before, 7 genes were found to be upregulated in breast muscle and 8 were upregulated in heart tissue at the transcriptional level.

↑ Breast Muscle	↑ Heart
ACTA1	ACTC1
GAPDH	FABP3
LDHA	FTH1
MYL1	MYH15
TNNI2	MYL10
TNNT3	MYL2
TPM1	MYL3
	TNNT2

Table 5.2: List of genes that were upregulated in breast muscle or cardiac muscle when compared to the other tissue.

Of the genes that were found to be upregulated in the breast muscle, 6 of them were also upregulated in comparison to all other tissues studied. One gene (ACTA1) had the largest difference in expression levels between the two tissues, but was not identified as a major component of the variation between breast muscle and all other tissues. This gene, actin alpha 1, is specifically noted as belonging to skeletal muscle (Gineste, et al. 2013). Conversely, one of the genes highly upregulated in the heart is another type of actin: actin, alpha, cardiac muscle 1 (ACTC1). The difference in which type of actin is expressed appears to be indicative of a large amount of the variation between the skeletal and cardiac muscles.

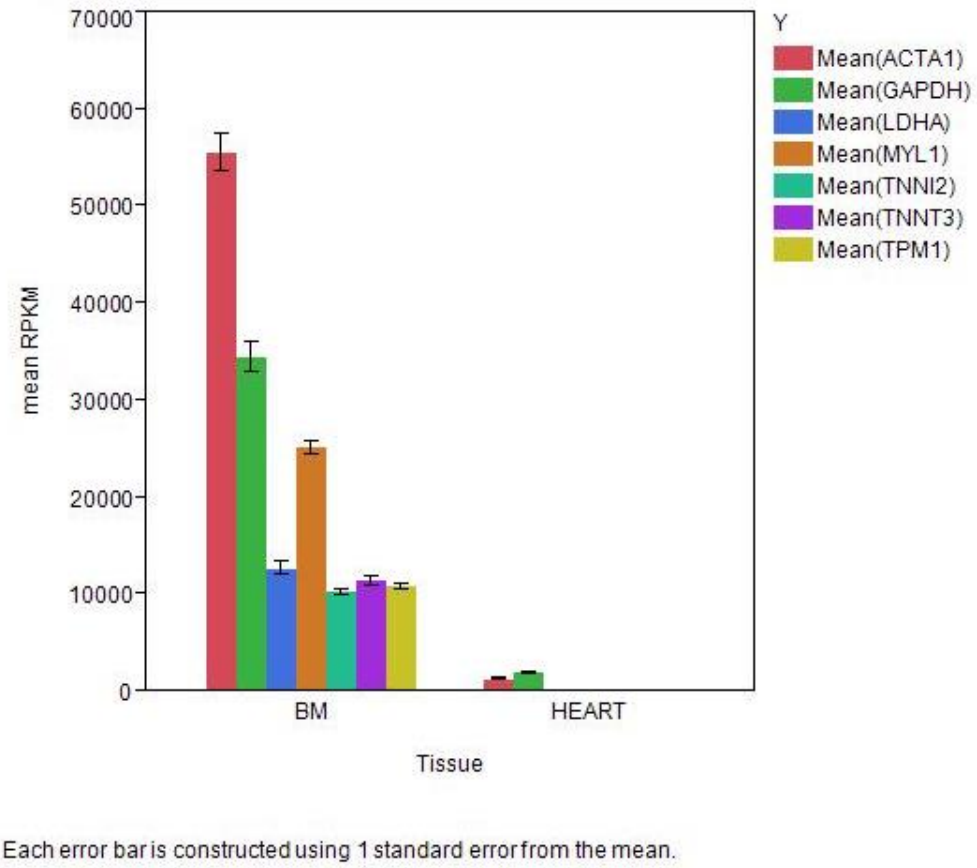

Figure 5.8: Comparison of the gene expression levels of genes found to be upregulated in breast muscle samples versus heart tissue.

Other major differences arise in the specific variants of troponin and myosin present in each muscle type. The breast muscle samples are rich in MYL1 (myosin light chain 1) while the heart utilizes MYL2, MYL3, MYL10, and MYH15 (myosin light chains 2, 3, 10; myosin heavy chain 15). MYL2 in particular is specifically noted as belonging to cardiac muscle (Wang, et al. 2013), but MYL3 is tagged as derived from both cardiac muscle (Andersen, et al. 2012) and skeletal muscle (Zhang, et al. 2010). Breast muscle samples had larger amounts of two troponins (TNNI2 and TNNT3) while the heart had a different type of troponin T

(TNNT2) specifically denoted as cardiac in origin (Hirtle-Lewis, et al. 2013). The heart also has a large presence of FTH1 (ferritin).

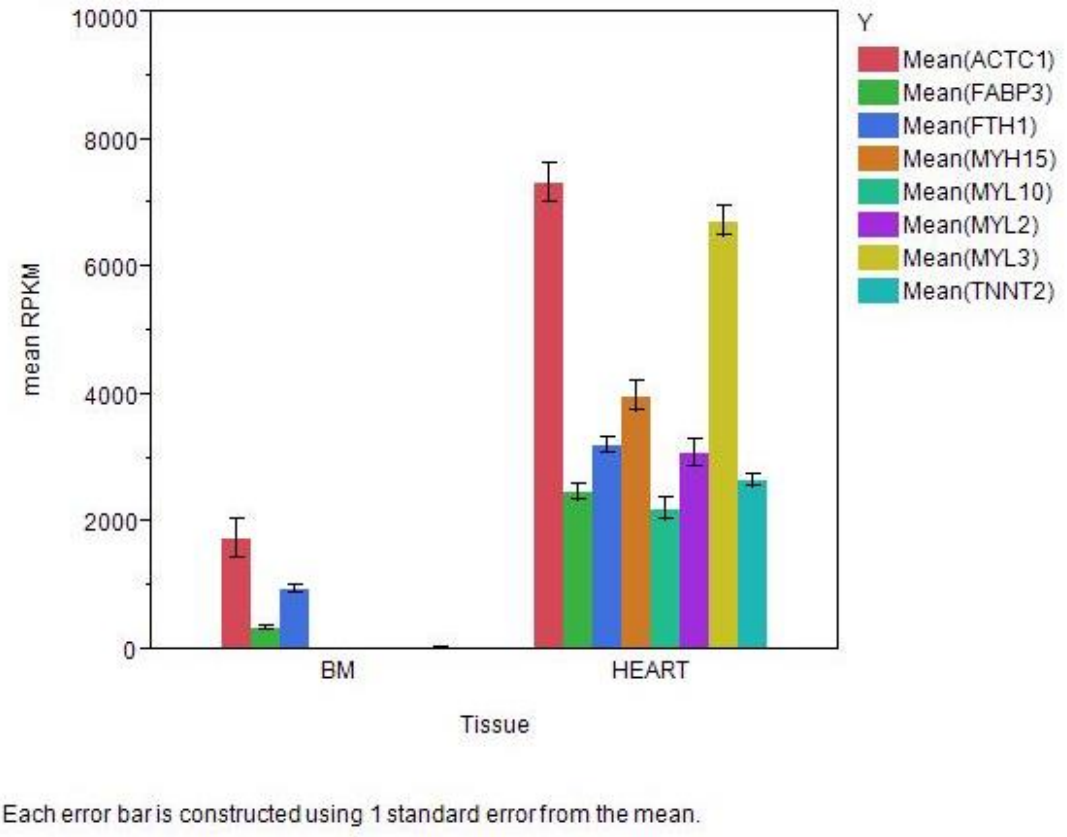

Figure 5.9: Comparison of the gene expression levels of genes found to be upregulated in cardiac tissue samples versus breast muscle.

5.4 Liver and Duodenum

The liver and duodenum clustered together in the dendrogram, indicating that their transcriptomes are more related to each other than to any of the other tissues in the study. Using the principle component analysis as before, 6 genes were found that influenced the separation of the liver and duodenum: 2 upregulated in liver and 4 upregulated in duodenum.

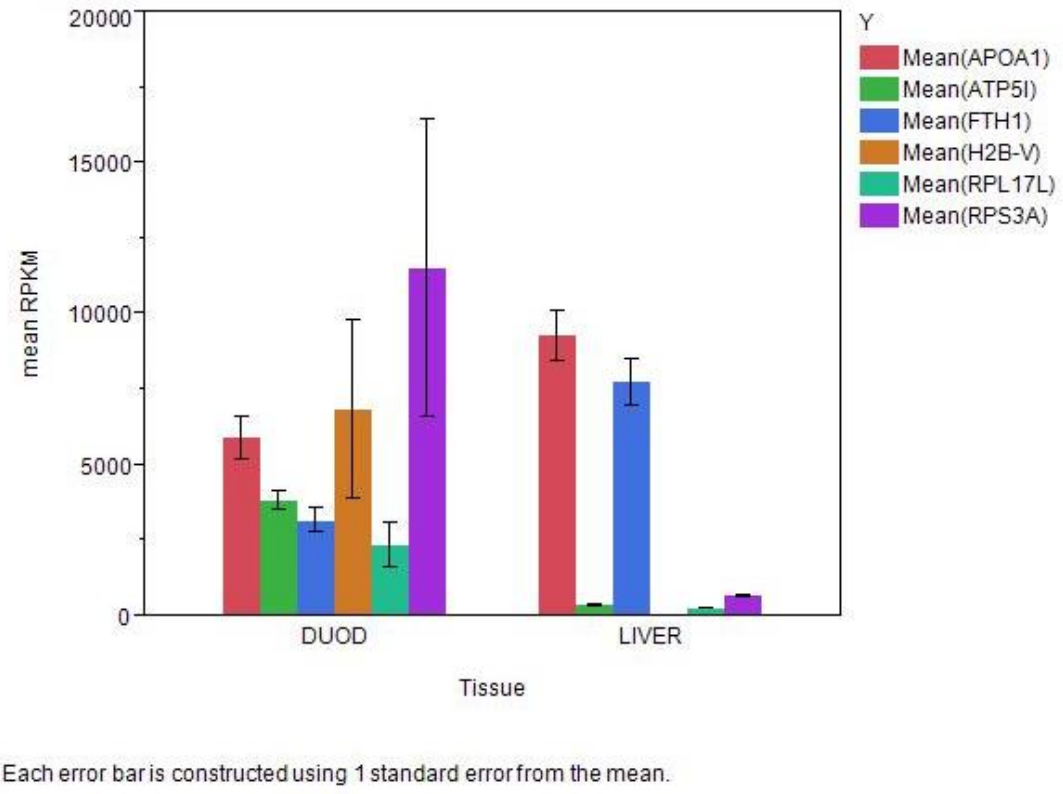

Figure 5.10: Comparison of the gene expression levels in duodenum and liver samples for 6 genes found to be differentially expressed between the two tissues.

The genes upregulated in the liver samples – APOA1 and FTH1 – encode an apolipoprotein and ferritin, respectively. Apolipoproteins bind lipids to form lipoproteins for transport through the lymphatic and circulatory systems. Given that one of the major roles of the liver is known to be lipid metabolism, the increased presence of a gene for an apolipoprotein comes as no surprise. Additionally, the liver is a major site of iron storage in the body, which is usually mediated by ferritin, explaining that gene's presence as well. The duodenal genes, however, are more difficult to explain. RPL17L and RPS3A code for ribosomal proteins, ATP5I is an ATP synthase, and H2B-V is a histone cluster.

5.5 Cerebellum

Seven genes were identified that were upregulated in cerebellum when compared to all other tissues. These included CALM (calmodulin 1), CST3 (cystatin C), HSPA8 (heat shock cognate), OAZ1 (ornithine decarboxylase antizyme), STMN1 (stathmin), THY1 (T-cell antigen), and VSNL1 (visinin-like protein 1).

Calmodulin (CaM) is a calcium-binding messenger protein that confers calcium regulation on a large number of second messenger systems. The calcium/calmodulin complex regulates a family of kinases (Ca^{2+}/calmodulin-dependent kinases II or CaMKII) which are believed to be important mediators of long-term potentiation (LTP) (Salerno, et al. 2012). LTP is initiated when N-methyl-D-aspartate (NMDA) receptors allow an influx of Ca^{2+} into the post-synaptic neuron, which in turn activates CaMKII (Hopper and Garthwaite, 2006; Rycroft and Gibb, 2002). CaMKII has also been shown to bind to NMDA receptors directly and inhibit NMDA activation in a calcium-rich environment (Gardoni, et al. 2001).

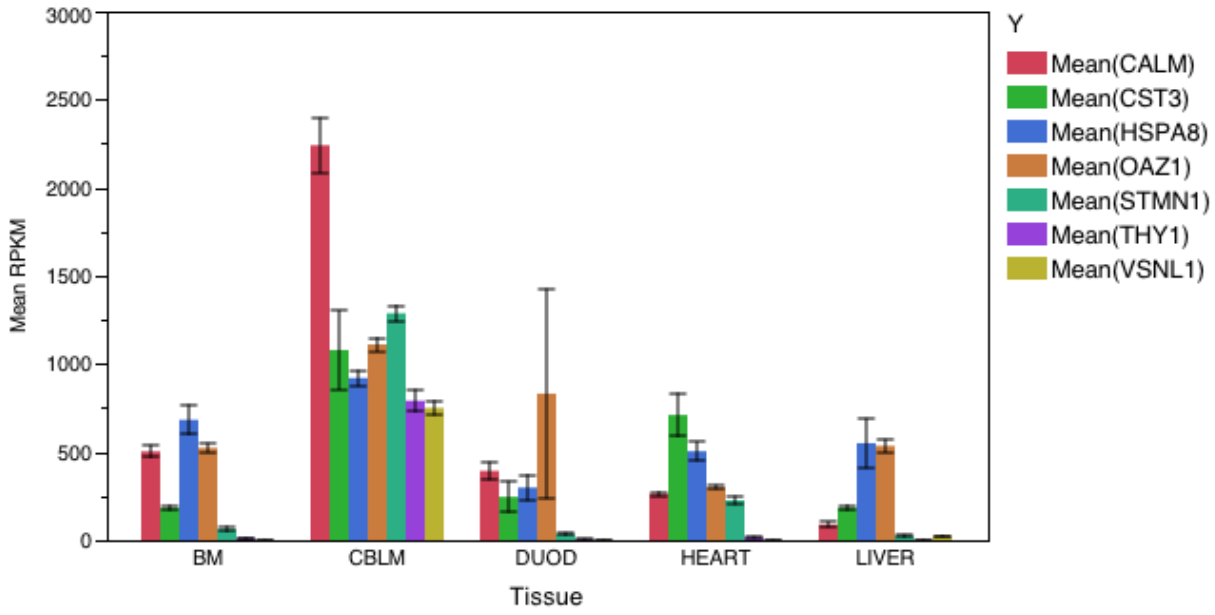

Figure 5.11: Comparison of the gene expression levels for 7 genes found to be upregulated in cerebellum compared to all other tissues.

Cystatin C (encoded by CST3) is an inhibitor of cysteine proteases known as cathepsins, many of which are implicated in neurodegenerative disorders and brain tumors. Mutations of CST3 cause the resulting protein to become less stable and prone to aggregation into amyloid plaques which lead to stroke, dementia, and brain hemorrhage (Olaffson et al., 1996; Palsdottir et al., 2006). Release of lysosomal cathepsins into the cytosol has been observed as a response to cellular damage or stress and occurs just before cell death (Windleborn and Lipton, 2008). Inhibitors of cathepsins seem to mitigate the cellular damage in the event of release from the lysosome.

Stathmin (STMN1) is an inhibitor of microtubule formation and it has been observed at high concentrations within the mouse amygdala. Stathmin-knockout mice displayed significant reductions in both innate and learned fear responses (Shumyatsky, et al., 2005) as

well as impaired innate maternal behavior, but enhanced adult social interaction behavior (Martel, Nishi, and Shumyatsky, 2008). Regulation of microtubule structure is critical for the development of neural networks through sufficient dendrite arborization (Ohkawa, et al., 2007). Reduction in gene expression and downregulation by CaMKII in early cerebellar development prevents microtubule destabilization and allows for dendrite growth. Overexpression of stathmin limits dendritic length and number, reducing the connectivity of the neural network. Extreme inhibition of stathmin similarly slows dendritic outgrowth, suggesting that a correct balance between microtubule polymerization and depolymerization is critical for optimal neuronal growth.

Ornithine decarboxylase antizyme (OAZ1) binds and inhibits the action of ornithine decarboxylase (ODC) which is a catalyst of polyamine biosynthesis (Kilpeläinen et al., 2000). In particular, ODC catalyzes the decarboxylation of ornithine to form putrescine. Putrescine is further converted into spermidine and finally spermine, all of which have been shown to inhibit the action of nNOSs (Sojanović et al, 2010). The three polyamines share similar structural features with L-arginine, the nNOS substrate (Hu, Mahmoud, and El-Fakahany, 1994). Therefore, the antizyme encoded by OAZ1 inhibits the formation of polyamines and could enhance the performance of nNOSs along with calmodulin.

Visinin-like protein 1 (VSNL1) is a calcium-sensor protein that associates with membranes in a calcium-dependent manner (Li et al, 2011). It modulates intracellular signaling pathways of the central nervous system (Burgoyne, 2007) by regulating adenylyl cyclase (which gives rise to cyclic AMP) and guanylyl cyclase (which gives rise to cyclic GMP). The cyclic monophosphates act as second messengers to relay surface signals to internal structures. In particular, cGMP activates calcium channels and allows ions into the

cell. VSNL1 is suspected to be involved in the pathophysiology of Alzheimer's disease due to association with amyloid plaques (Schnurra et al., 2001).

HSPA8 is a consitutively expressed heat shock cognate in the HSP70 family. It binds to newly synthesized polypeptide strands to facilitate correct folding and conformation (Stricher et al., 2013). In the nervous system, HSPA8 works with auxilin and synaptojanin as an ATPase to remove clathrin coatings from vesicles.

THY1 is a membrane glycoprotein T-cell antigen that is strongly expressed in mature axons (Rege and Hagood, 2006). Its function is not fully known, but it is developmentally regulated; THY1 levels are low at infancy and increase into adulthood. Knockout mice display normal social interactions and maze learning skills, but fail to learn from social cues and companions' actions.

Chapter 6

CONCLUSIONS

These comparisons between Heritage and Ross tissue morphometrics and gene expression patterns provide a starting point for understanding how human-directed evolution has affected these lines of chickens. One significant difference between the lines manifests in the breast muscle, which has a higher growth rate and allometric coefficient in the Ross birds. This improvement in muscle yield in the Ross line may be supported by changes in the growth of other tissues. One organ that appears to have changed is the small intestine. The Ross birds have significantly longer normalized small intestines than the Heritage birds. The increased length likely provides additional surface area supporting the increased feed efficiency noted in the Ross line compared to the Heritage (Schmidt, et al. 2009). This improvement in nutrient absorption provides the additional energy needed to support the rapid growth of the breast muscle.

The energy needed for rapid muscle growth could also be provided by diverting energy from other organs. A previous study (Schmidt, et al. 2009) concluded that there was a significant difference in cardiac growth between the two lines; in this study the differences in heart size between the two lines was not as dramatic. One possible source of the difference between the studies could be the way in which the birds were raised. In the original study, birds were raised in cages, while in the current work the birds were raised in open floor houses. It is

conceivable that the exercise provided by the greater ability to move about in the houses provided for additional heart growth.

Two organs not previously compared between the Ross and Heritage lines were the spleen and brain. Both of these organs are significantly smaller in birds from the Ross line compared to those from the Heritage line. The most striking difference in allometric coefficients was between the Ross and Heritage spleens (Heritage: 8.1; Ross: 6.0). Also higher in the Heritage line was the brain allometric coefficient (Heritage: 1.3; Ross 1.1). These data indicate that the spleen and brain are smaller organs in the Ross birds compared to Heritage (when normalized for total bird mass) and this finding supports the hypothesis that the increased breast muscle growth in the Ross birds may lead to reduced growth in other organs, such as the brain and spleen. Energy saved by reducing the growth of the brain and spleen could be used to support the additional growth of the breast muscle.

The study succeeded in identifying a small number of genes that appear to be integral to the unique function of certain tissues. The breast muscle had the highest expression of glycolytic pathway genes than any other tissue studied. Skeletal muscle and cardiac muscle are distinct from one another by expressing different types of contractile elements. The liver is characterized by expression of apolipoproteins and ferritin, and the cerebellum has various neuron-specific proteins. Future work focusing on individual tissues or smaller sets of tissues would be able to glean more specific pathways and functional groups. Similarly, all of the analysis presented only used known coding genes from the most current version of the chicken genome at the time. New genes could be discovered that cause greater divergence in character between the tissues and their functions, leading to further understanding of the complexities of living systems.

REFERENCES

Andersen, P. S., P. L. Hedley, S. P. Page, P. Syrris, J. C. Moolman-Smook, W. J. McKenna, P. M. Elliott, and M. Christiansen. 2012. A novel myosin essential light chain mutation causes hypertrophic cardiomyopathy with late onset and low expressivity. Biochem. Res. Int. 2012:685108.

Burgoyne, R. D. 2007. Neuronal calcium sensor proteins: generating diversity in neuronal Ca^{2+} signaling. Nat. Rev. Neurosci. 8(3):182-193.

Cheema, M. A., M. A. Qureshi, and G. B. Havenstein. 2003. A comparison of the immune response of a 2001 commercial broiler with a 1957 randombred broiler strain when fed representative 1957 and 2001 broiler diets. Poult. Sci. 82:1519-1529.

Fumihito, A., T. Miyake, S. Sumi, M. Takada, S. Ohno, and N. Kondo. 1994. One subspecies of the red junglefowl (*Gallus gallus gallus*) suffices as the matriarchic ancestor of all domestic breeds. Proc. Natl. Acad. Sci. USA 91:12505-12509.

Gardoni, F., L. H. Schrama, A. Kamal, W. H. Gispen, F. Cattabeni, and M. Di Luca. 2001. Hippocampal synaptic plasticity involves competition between Ca^{2+}/calmodulin-dependent protein kinase II and postsynaptic density 95 for binding to the NR2A subunit of the NMDA receptor. J. Neurosci. 21(5):1501-1509.

Gineste, C., G. Duhamel, Y. Le Fur, C. Vilmen, P. J. Cozzone, K. J. Nowak, D. Bendahan, and J. Gondin. 2013. Multimodal MRI and ^{31}P-MRS investigations of the ACTA1(Asp286Gly) mouse model of nemaline myopathy provide evidence of impaired *in vivo* muscle function, altered muscle structure and disturbed energy metabolism. PLoS ONE 8(8): e72294.

Griffin, H. D., and C. Goddard. 1994. Rapidly growing broiler (meat-type) chickens: Their origin and use for comparative studies of the regulation of growth. Int. J. Biochem. 26:19-28.

Havenstein, G .B., P. R. Ferket, and M. A. Qureshi. 2003. Carcass composition and yield of 1957 versus 2001 broilers when fed representative 1957 and 2001 broiler diets. Poult. Sci. 82(10):1509-18.

Havenstein, G. B., P. R. Ferket, S. E. Sheideler, and D. V. Rives. 1994. Carcass composition and yield of 1991 vs 1957 broilers when fed "typical" 1957 and 1991 broiler diets. Poult. Sci. 73(12):1795-804.

Havenstein, G. B., P. R. Ferket, and M. A. Qureshi. 2003. Growth, livability, and feed conversion of 1957 versus 2001 broilers when fed representative 1957 and 2001 broiler diets. Poult. Sci. 82(10):1500-8.

Hirtle-Lewis, M., K. Desbiens, I. Ruel, N. Rudzicz, J. Genest, J. C. Engert, and N. Gianetti. 2013. The genetics of dilated cardiomyopathy: a prioritized candidate gene study of *LMNA, TNNT2, TCAP,* and *PLN*. Clin. Cardiol. 36:628-633.

Hopper, R. A., and J. Garthwaite. 2006. Tonic and phasic nitric oxide signals in hippocampal long-term potentiation. J. Neurosci. 26(45):11513-11521.

Hu, J., M. I. Mahmoud, and E. E. El-Fakahany. 1994. Polyamines inhibit nitric oxide synthase in rat cerebellum. Neurosci. Lett. 175:41-45.

Ignatova, T. N., Kukekov, V. G., Laywell, E. D., Suslov, O. N., Vrionis, F. D. and Steindler, D. A. (2002), Human cortical glial tumors contain neural stem-like cells expressing astroglial and neuronal markers in vitro. Glia, 39: 193–206.

Kanginakudru, S., M. Metta, R. D. Jakati, and J. Nagaraju. 2008. Genetic evidence from Indian red jungle fowl corroborates multiple domestication of modern day chicken. BMC Evol. Biol. 8:174.

Kilpeläinen, P., E. Rybnikova, O. Hietala, and M. Pelto-Huikko. 2000. Expression of ODC and its regulatory protein antizyme in the adult rat brain. J. Neurosci. Res. 62(5):675-685.

Komiyama, T., K. Ikeo, Y. Tateno, and T. Gojobori. 2004. Japanese domesticated chickens have been derived from Shamo traditional fighting cocks. Mol. Phylogenet. Evol. 33:16-21.

Konarzewski, M., A. Gavin, R. McDevitt, and I. R. Wallis. 2000. Metabolic and organ mass responses to selection for high growth rates in the domestic chicken (*Gallus domesticus*). Physiol. Biochem. Zool. 73:237-248.

Li, C., W. Pan, K. H. Braunewell, and J. B. Ames. 2011. Structural analysis of Mg2+ and Ca 2+ binding, myristoylation, and dimerization of the neuronal calcium sensor and visinin-like protein 1 (VILIP-1). J. Biol. Chem. 286(8):6354-66.

Lilburn, M. S. 1994. Skeletal growth of commercial poultry species. Poult. Sci. 73:237-248.

Martel, G., A. Nishi, and G. P. Shumyatsky. 2008. Stathmin reveals dissociable roles of the basolateral amygdala in parental and social behaviors. 105(38):14620-14625.

McDevitt, R. M., G. Gm McEntee, and K. A. Rance. 2006. Bone breaking strength and apparent metabolisability of calcium and phosphorus in selected and unselected broiler chicken genotypes. Br. Poult. Sci. 47:613-621.

Morris, M. P. 1992. Ascites in broilers. Poult. Inst. October:26-32.

Ohkawa, N., K. Fujitani, E. Tokunaga, S. Furuya, and K. Inokuchi. 2007. The microtubule destabilizer stathmin mediates the development of dendritic arbors in neuronal cells. J. Cell Sci. 120:1447-1456.

Olaffson, I., L. Thorsteinsson, and O. Jensson. 1996. The molecular pathology of hereditary cystatin C amyloid angiopathy causing brain hemorrhage. Brain Pathol. 6(2):121-6.

Olkowski, A. A., C. Wojnarowicz, S. Nain, B. Ling, J. M. Alcorn, and B. Laarveld. 2008. A study on pathogenesis of sudden death syndrome in broiler chickens. Res. Vet. Sci. 85:131-140.

Palsdottir, A., A. O. Snorradottir, and L. Thorsteinsson. 2006. Hereditary cystatin C amyloid angiopathy: genetic, clinical, and pathological aspects. Brain Pathol. 16(1):55-9.

Ramsköld, D., E. T. Wang, C. B. Burge, R. Sandberg. 2009. An abundance of ubiquitously expressed genes revealed by tissue transcriptome sequence data. PLoS Comput Biol 5(12): e1000598.

Rath, N. C., G. R. Huff, W. E. Huff, and J. M. Balog. 2000. Factors regulating bone maturity and strength in poultry. Poult. Sci. 79:1024-1032.

Reddy, P. R. K., and P. B. Siegel. 1976. Selection for body weight at eight weeks of age. Egg production in relaxed and selected lines. Poult. Sci. 56:673-686.

Rege, T. A., and J. S. Hagood. 2006. Thy-1 as a regulator of cell-cell and cell-matrix interactions in axon regeneration, apoptosis, adhesion, migration, cancer, and fibrosis. FASEB J. 20(8):1045-1054.

Rycroft, B. K. and A. J. Gibb. 2002. Direct effects of calmodulin on NMDA receptor single-channel gating in rat hippocampal granule cells. J. Neurosci. 22(20):8860-8868.

Salerno, J. C., K. Ray, T. Poulos, H. Li, and D. K. Ghosh. 2012. Calmodulin activates neuronal nitric oxide synthase by enabling transitions between conformational states. FEBS Lett. 587(1):44-47.

Schmidt, C. J., M. E. Persia, E. Feierstein, B. Kingham, and W. W. Saylor. 2009. Comparison of a modern broiler line and a heritage line unselected since the 1950s. Poult. Sci. 88:2610-2619.

Schnurra, I., H. G. Bernstein, P. Riederer, and K. H. Braunewell. 2001. The neuronal calcium sensor protein VILIP-1 is associated with amyloid plaques and extracellular tangles in Alzheimer's disease and promotes cell death and tau phosphorylation *in vitro*: a link between calcium sensors and Alzheimer's disease? Neurobiol. Dis. 8(5):900-909.

Schoettle, C. E., E. F. Reber, J. O. Alberts, and H. M. Scott. 1956a. A study of New Hampshire x Barred Cloumbian chicks from two days of age to ten weeks of age. Poult. Sci. 35:95-98.

Schoettle, C. E., E. F. Reber, H. W. Norton, and J. O. Alberts. 1956b. A study of New Hampshire x Barred Columbian chicks from two days of age to ten weeks of age: Effects of coccidostats. Poult. Sci. 35:596-599.

Shumyatsky, G. P., G. Malleret, R.M. Shin, S. Takizawa, K. Tully, E. Tsvetkov, S. S. Zakharenko, J. Joseph, S. Vronskaya, D. Yin, U. K. Schubart, E. R. Kanel, and V. Y. Bolshakov. 2005. *Stathmin*, a gene enriched in the amygdala, controls both learned and innate fear. Cell. 123(4):697-709.

Stojanović, I., A. Jelenković, I. Stevanović, D. Pavlović, G. Bjelaković, and T. Jevtović-Stoimenov. 2010. Spermidine influence on the nitric oxide synthase and arginase activity relationship during experimentally induced seizures. J. Basic Clin. Physiol. Pharmacol. 21(2):169-85.

Stricher, F., C. Macri, M. Ruff, and S. Muller. 2013. HSPA8/HSC70 chaperone protein: structure, function, and chemical targeting. Autophagy. 9:0-17.

Thomas, C. H., W. L. Blow, C. C. Cockerham, and E. W. Glazener. 1958. The heritability of body weight, gain, feed consumption and feed conversion in broilers. Poult. Sci. 37:862-869.

Wang, M., Q. Yu, L. Wang, and H. Gu. 2013. Distinct patterns of histone modifications at cardiac-specific gene promoters between cardiac stem cells and mesenchymal stem cells. Am. J. Physiol. – Cell Ph. 304:C1080-C1090.

Waterhouse, H. N., and H. M. Scott. 1962. Effect of sex, feathering, rate of growth and acetates on the chick's need for glycine. Poult. Sci. 41:1957-1984.

Windleborn, J. A., and P. Lipton. 2008. Lysosomal release of cathepsins causes ischemic damage in the rat hippocampal slice and depends on NMDA-mediated calcium influx, arachidonic acid metabolism, and free radical production. J. Neurochem. 106(1):56-69).

Zhang, Q., H.G. Lee, J.A. Han, E. B. Kim, J. Yin, M. Baik, Y. Shen, S.H. Kim, K.S. Seo, and Y.J. Choi. 2010. Differentially expressed proteins during fat accumulation in bovine skeletal muscle. Meat Sci. 86(3):814-820.

Appendix A

AACUC APPROVAL FORM

UNIVERSITY OF DELAWARE

COLLEGE OF AGRICULTURE AND NATURAL RESOURCES

AGRICULTURAL ANIMAL CARE AND USE COMMITTEE

Application for Use of Agricultural Animals

In Teaching or Research

AACUC Protocol Number: (27) 12-22-10R

TITLE OF PROJECT: Scientific Investigation into the response of Broiler Chickens to heat stress by transcriptome analysis

INSTRUCTOR/PRINCIPAL INVESTIGATOR: Carl Schmidt

New or Three Year Review (mark one)

NEW X□ **THREE YEAR □**

If this is a 3 year renewal, what is the assigned existing protocol number?
_____

(This section for Committee use only)

Application Approved (date): 1-5-2011

Application Rejected (date): _____

Reason for Rejection: _____

Signature, Animal Care and Use Committee **1-5-2011 Date**

APPLICATION INFORMATION:

Title: Scientific Investigation into the response of Broiler Chickens to heat stress by transcriptome analysis

Principal Investigator(Research): Carl J. Schmidt

Address: 107 Allen Lab, 601 Sincock Lane, University of Delaware, Newark, Delaware 19716

Telephone: (302)-831-1334 Email: schmidtc@udel.edu

Proposed start date: February 1 2011 End date: January 31, 2014

Teaching/Outreach □ Research X

If TEACHING box was checked, select from the following:

Demonstration □ Laboratory □ Student Project □

If student project, please define project: _____

Have all participants listed above reviewed the application and is familiar with the proposed work?

YES X□ NO □

If no, identify those needing to review application.

_____ _____ _____

Are all proposed animal care management procedures 1) defined as "pre-approved" by the Animal Care and Use Committee, or 2) part of the Standard Operating Procedures developed by the Animal Care and Use Committee for that particular species?

YES X□ NO □ To be determined by AACUC □

Have all participants been trained? YES X□ NO □

Which participants have not been trained?

_____ _____ _____

Name the person responsible for conducting the training.

If after hours participation is required by students, please describe how this is being handled. (e.g. supervisors, assistants, etc.) Please include the times and days that students may be on site.

ANIMAL INFORMATION:

Common Name of the Animal Requested: Chickens

Amount Being Requested: 1600

Source of Animals: Allen Family Foods and Chet Utterback at the University of Illinois

Where are the animals being held: UD Poultry Farm

Briefly Describe the Goals or Objectives of this Application (use additional space as needed).

The goal of this study is to determine the ability of the modern broiler chicken to handle heat stress compared to the heritage variety. Following treatment, birds will be euthanized by cervical dislocation and organs harvested for transcriptome analysis.

Rationale for scale of study: This is a new area of research, using new genomic approaches to understand how birds respond to heat stress. The large numbers of birds are necessitated in order to achieve statistical significance in our gene mapping studies.

Birds: Heritage birds will be obtained from Chet Utterback at the University of Illinois and the Ross708 birds from a local supplier. Birds will be wing tagged and randomly placed into control and experimental groups as described below (Heat Shock Scheme). In each experiment 100 birds from each line will be included in each experimental group. The size of the facilities at the University of Delaware limit the number of birds per chamber, hence we anticipate multiple replicates over time to a total of 1600 birds per line. Blood will be taken from each bird for DNA extraction prior to heat stress. Also, 12 birds from each group will be removed on post hatch days 2, 7 and 21, euthanized (cervical dislocation) and tissues harvested. Blood biomarker data using the iSTAT will be collected from these birds prior to euthanasia. Chambers will be monitored on a daily basis to insure adequate feed and water and to remove any sick or dead birds.

Heat Shock Scheme: Controls are hatched from eggs incubated at 37^{o}C (99^{o}F) while thermal conditioned embryos will be incubated at 39.6^{o}C (103^{o}F) from embryonic days 10-18, then returned to 37^{o}C. Following hatch through day 21, they will be kept at ambient temperatures. At day 22, the original Control birds will be split into two populations (Control A and B) and the *In Ovo* Heat-conditioned bird also split into two groups (*In Ovo* Heat Conditioned A and B). The A populations will be kept at ambient temperatures while the B populations will be heat stressed at 35^{o}C (95^{o}F) or 7 hours per day for 21 days. There will be 20 birds per chamber. Multiple replicates (hatches) will be conducted. At the end of the trial (6 weeks from hatch), birds will be euthanized and tissues collected.

Attached below is additional protocol information.

Does this procedure involve surgery? YES NO X□

If yes, explain in detail the surgery.

Are drugs, vaccines and/or medications being used? YES □ NO X□

If yes, describe what is being used. Include dosages and routes of administration.

How often are animals monitored and how are sick or injured animals being handled?

The birds will be checked daily and given food and fresh water *ad libidum*. Sick or injured animals will be euthanized by cervical dislocation.

What is the method of euthanasia, if specified in the protocol?

Cervical dislocation as per AVMA Guidelines on Euthanasia 2007

List the veterinarian who is on-call:

Name: Miguel Ruano Telephone: 302-831-1539

Does this application require approval from Occupational Health & Safety (OHS)?
YES □ NO X□

If yes, what form(s) are attached?_____

NOTE: OHS approval is required for experiments involving the use of hazardous substances such as radioactive materials, highly toxic or carcinogenic materials, human reproductive hazards, or zoonotic or human pathogens.

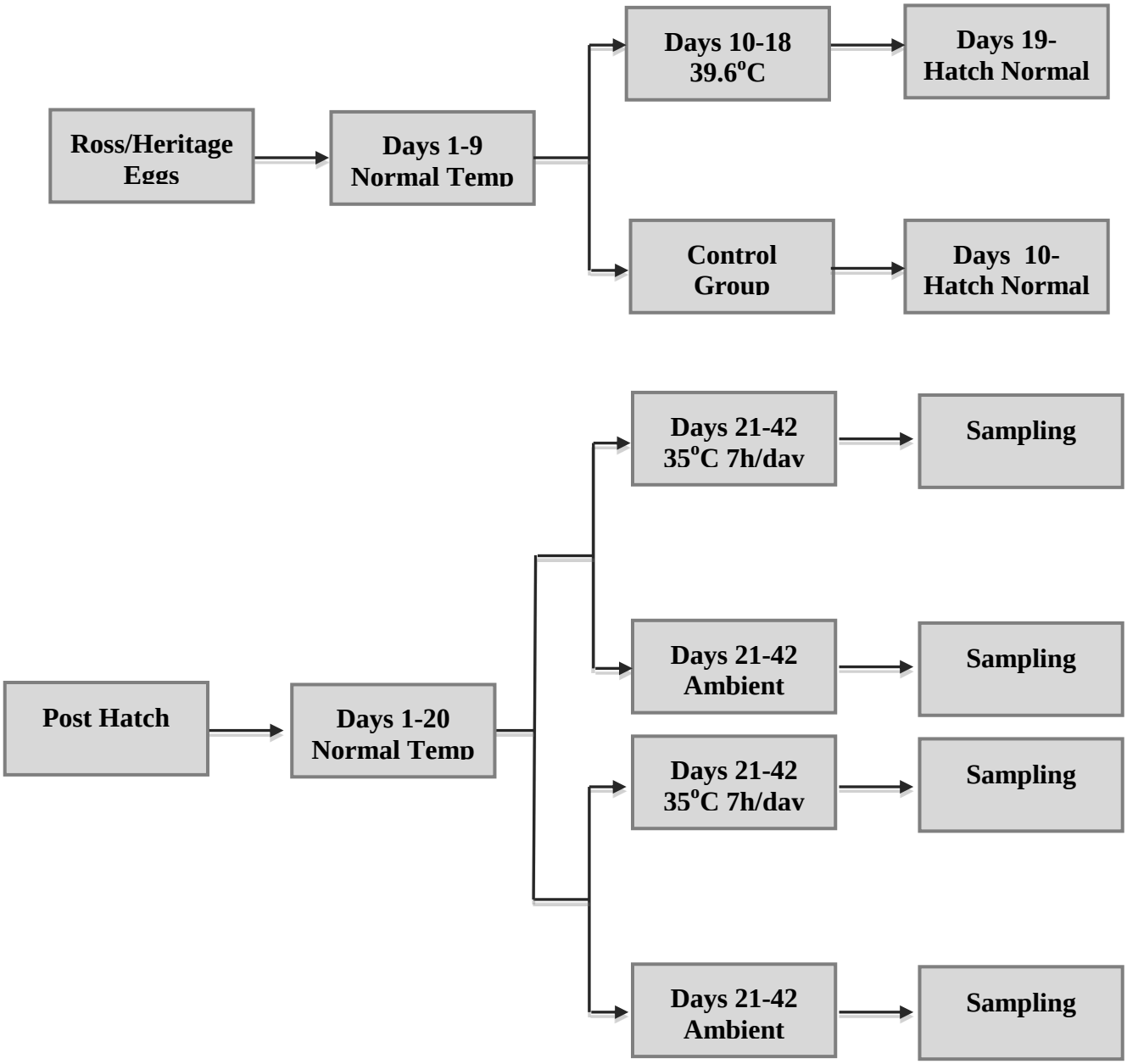

Ross Heritage heat stress experiment: Eggs will be either heat stressed or maintained as controls from embryonic days 10-18, and then returned to normal temperatures. Subsequently, both heat stressed and control birds will be split into two groups each, with one group heat stressed from days 21-42 post-hatch, with the second group kept at ambient temperatures to function as a control. So, there will be a total of 8 groups at the end of each experiment.

Tissue Samples: Genomic DNA & RNA:

- Blood
- Brain
- Heart
- Liver
- Duodenum
- Jejunum
- Ileum
- Large Intestine
- Ceca (and contents)
- Fat pad
- Breast muscle
- Spleen

Weekly Measurements:

- iSTAT metabolic measurements
- Weight

Day 21/42

- Shank length
- Shank Width

Morphometric:

- Liver
- Spleen
- Duodenum
- Jejunum
- Ileum
- Large Intestine
- Breast muscle
- Heart

Samples are needed for:

- RNAseq

- microRNA
- Genomic DNA
    - SNP
    - CVN
    - Epigenetics

Appendix B

RPKM VS CT DATA

Sample	Ct	RPKM	Log2RPKM
TDRD1	31.5015	0.08	-3.64386
TDRD1	31.5758	0.08	-3.64386
TDRD1	31.1804	0.08	-3.64386
SLC12A1	32.0169	0.03	-5.05889
SLC12A1	31.9069	0.03	-5.05889
SLC12A1	31.5336	0.03	-5.05889
IMPG1	34.0989	0.11	-3.18442
IMPG1	34.0775	0.11	-3.18442
IMPG1	33.5613	0.11	-3.18442
IKZF1	35.4036	0.09	-3.47393
IKZF1	36.545	0.09	-3.47393
IKZF1	33.6673	0.09	-3.47393
FSD2	34.1743	0.06	-4.05889
FSD2	33.6605	0.06	-4.05889
FSD2	33.8068	0.06	-4.05889
BIRC7	29.0966	0.47	-1.08927
BIRC7	29.0574	0.47	-1.08927
BIRC7	29.1731	0.47	-1.08927
FOXL2	32.2746	0.48	-1.05889
FOXL2	32.4554	0.48	-1.05889
FOXL2	32.5179	0.48	-1.05889
EXDL1	28.9332	0.73	-0.45403
EXDL1	29.157	0.73	-0.45403
EXDL1	29.0493	0.73	-0.45403
C10orf12	32.5458	1.03	0.042644
C10orf12	32.2486	1.03	0.042644
C10orf12	32.0427	1.03	0.042644
TWISTNB	26.0516	3.13	1.646163
TWISTNB	26.0692	3.13	1.646163

Sample	Ct	RPKM	Log2RPKM
TWISTNB	26.0275	3.13	1.646163
SLC15A2	30.9272	3.84	1.941106
SLC15A2	31.325	3.84	1.941106
SLC15A2	31.8894	3.84	1.941106
GPCPD1	26.9802	5.11	2.353323
GPCPD1	27.049	5.11	2.353323
GPCPD1	26.5925	5.11	2.353323
C3H6orf129	26.508	5.3	2.405992
C3H6orf129	26.8155	5.3	2.405992
C3H6orf129	26.8908	5.3	2.405992
DDHD1	25.1482	7.42	2.891419
DDHD1	25.1246	7.42	2.891419
DDHD1	24.9668	7.42	2.891419
ZFYVE21	26.4223	6.56	2.713696
ZFYVE21	26.6012	6.56	2.713696
ZFYVE21	26.4597	6.56	2.713696
C7orf50	25.5776	10.02	3.324811
C7orf50	25.5491	10.02	3.324811
C7orf50	25.459	10.02	3.324811
GLRA4	29.8753	10.64	3.411426
GLRA4	30.3932	10.64	3.411426
GLRA4	30.3239	10.64	3.411426
CNBP	21.2405	150.43	7.232949
CNBP	21.1269	150.43	7.232949
CNBP	21.0927	150.43	7.232949
GBAS	24.5607	53.98	5.754353
GBAS	24.8104	53.98	5.754353
GBAS	25.1905	53.98	5.754353
HNRNPAB	24.575	69.06	6.109778
HNRNPAB	24.4822	69.06	6.109778
HNRNPAB	24.2123	69.06	6.109778
KLHDC2	23.3419	94.57	6.563311
KLHDC2	23.5594	94.57	6.563311
KLHDC2	23.5688	94.57	6.563311
NDUFA4	20.0731	206.61	7.690766
NDUFA4	20.0868	206.61	7.690766

Sample	Ct	RPKM	Log2RPKM
NDUFA4	20.0993	206.61	7.690766
SSR1	22.2925	75.72	6.242603
SSR1	22.3934	75.72	6.242603
SSR1	22.6305	75.72	6.242603
CASP1	18.8801	5.74	2.521051
CASP1	18.7064	5.74	2.521051
CASP1	20.1652	5.74	2.521051
CCT7	16.8878	79.08	6.305241
CCT7	16.5151	79.08	6.305241
CCT7	17.8017	79.08	6.305241
CDC42	14.5514	141.88	7.148527
CDC42	14.0779	141.88	7.148527
CDC42	14.3834	141.88	7.148527
GAPDH	14.8187	1380.24	10.4307
GAPDH	14.9848	1380.24	10.4307
GAPDH	15.0932	1380.24	10.4307
HMGB1	19.1442	112.97	6.819796
HMGB1	19.6274	112.97	6.819796
HMGB1	19.5293	112.97	6.819796
HSPB1	22.047	4.06	2.02148
HSPB1	21.7978	4.06	2.02148
HSPB1	18.5091	4.06	2.02148
LY96	22.1408	0.65	-0.62149
LY96	22.199	0.65	-0.62149
LY96	23.574	0.65	-0.62149
ODC1	19.685	17.6	4.137504
ODC1	19.3094	17.6	4.137504
ODC1	19.5153	17.6	4.137504
PANK1	19.8493	11.3	3.498251
PANK1	19.4574	11.3	3.498251
PANK1	20.522	11.3	3.498251
RPL4	14.1437	311.88	8.284847
RPL4	14.6648	311.88	8.284847
RPL4	14.1657	311.88	8.284847
RPL30	14.2	125.08	6.966707
RPL30	14.1735	125.08	6.966707

Sample	Ct	RPKM	Log2RPKM
RPL30	16.8728	125.08	6.966707
RPS6	15.2465	260.35	8.024309
RPS6	14.2649	260.35	8.024309
RPS6	14.1501	260.35	8.024309
RPS7	14.5741	71.06	6.150966
RPS7	15.0463	71.06	6.150966
RPS7	15.4662	71.06	6.150966
SPARC	16.7619	358.68	8.486553
SPARC	13.7798	358.68	8.486553
SPARC	15.1025	358.68	8.486553
TPT1	14.3952	724.16	9.500165
TPT1	14.2351	724.16	9.500165
TPT1	14.3145	724.16	9.500165
VPS13A	22.5839	1.24	0.31034
VPS13A	21.3995	1.24	0.31034
VPS13A	22.002	1.24	0.31034
VPS35	15.5527	30.88	4.948601
VPS35	19.065	30.88	4.948601
VPS35	15.3972	30.88	4.948601